AD-A127 805 TWO MODELS OF TIME CONSTRAINED TARGET TRAVEL BETWEEN TWO ENDPOINTS CONSTR.. (U) NAVAL POSTGRADUATE SCHOOL MONTEREY CA W J COMSTOCK MAR 83 1/2

UNCLASSIFIED F/G 12/1 NL

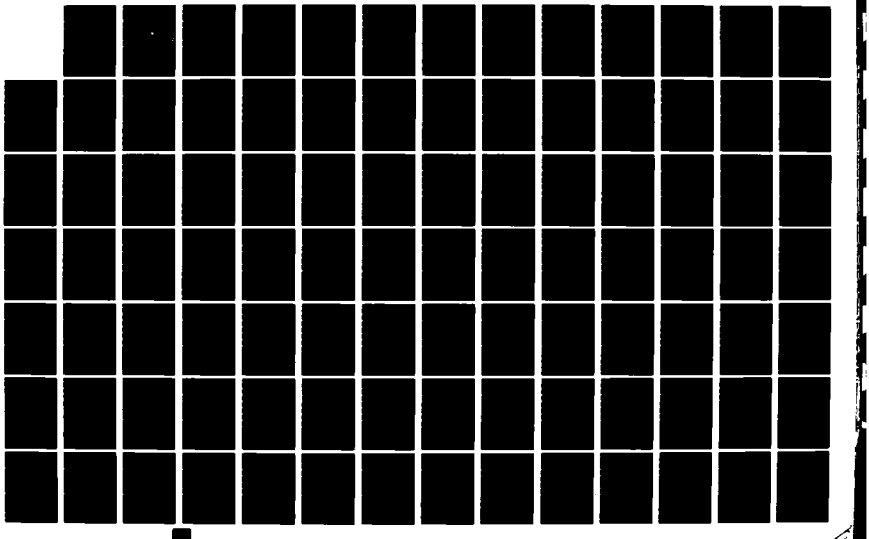

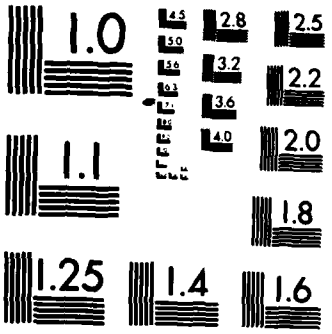

(2)

NAVAL POSTGRADUATE SCHOOL
Monterey, California

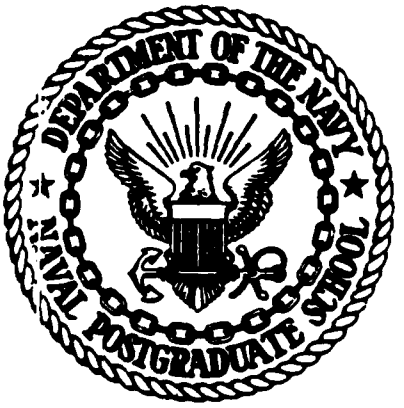

THESIS

TWO MODELS OF TIME CONSTRAINED TARGET TRAVEL BETWEEN TWO ENDPOINTS CONSTRUCTED BY THE APPLICATION OF BROWNIAN MOTION AND A RANDOM TOUR

by

William Justin Comstock

March 1983

Thesis Advisor: Donald P. Gaver

Approved for public release; distribution unlimited

UNCLASSIFIED

SECURITY CLASSIFICATION OF THIS PAGE (When Data Entered)

REPORT DOCUMENTATION PAGE		READ INSTRUCTIONS BEFORE COMPLETING FORM
1. REPORT NUMBER	2. GOVT ACCESSION NO.	3. RECIPIENT'S CATALOG NUMBER
4. TITLE (and Subtitle) Two Models of Time Constrained Target Travel Between Two Endpoints Constructed by the Application of Brownian Motion and a Random Tour		5. TYPE OF REPORT & PERIOD COVERED Master's Thesis March 1983
		6. PERFORMING ORG. REPORT NUMBER
7. AUTHOR(s) William Justin Comstock		8. CONTRACT OR GRANT NUMBER(s)
9. PERFORMING ORGANIZATION NAME AND ADDRESS Naval Postgraduate School Monterey, California 93940		10. PROGRAM ELEMENT, PROJECT, TASK AREA & WORK UNIT NUMBERS
11. CONTROLLING OFFICE NAME AND ADDRESS Naval Postgraduate School Monterey, California 93940		12. REPORT DATE March 1983
		13. NUMBER OF PAGES 111
14. MONITORING AGENCY NAME & ADDRESS(if different from Controlling Office)		15. SECURITY CLASS. (of this report) Unclassified
		15a. DECLASSIFICATION/DOWNGRADING SCHEDULE

16. DISTRIBUTION STATEMENT (of this Report)

Approved for public release; distribution unlimited

17. DISTRIBUTION STATEMENT (of the abstract entered in Block 20, if different from Report)

18. SUPPLEMENTARY NOTES

19. KEY WORDS (Continue on reverse side if necessary and identify by block number)

Random Tour
Brownian Motion
Target Motion
Constrained Target Motion
Controlled Time of Arrival
Time Constrained Motion
Target Drift

20. ABSTRACT (Continue on reverse side if necessary and identify by block number)

A target must choose a path between some origin and destination. The total travel time and the target speed are specified, and the target wishes to maximize the "randomness" of its track subject to the spatial and temporal constraints. Measures of effectiveness are developed against which the "randomness" of any path-producing method can reasonably be judged. Previous investigations into the scenario are reviewed and two models

DD FORM 1 JAN 73 1473 EDITION OF 1 NOV 65 IS OBSOLETE
S/N 0102-014-6601

UNCLASSIFIED
SECURITY CLASSIFICATION OF THIS PAGE (When Data Entered)

are developed, one using a random tour with drift and the other derived from Brownian motion. Statistics generated by Monte Carlo simulations for both models are compared. While the Brownian motion derived process is not always under perfect control of the constraints, if the timed arrival constraint may be slightly violated then that process performs better against the measures of effectiveness and is easier for a target to execute than is the random tour with drift.

Approved for public release, distribution unlimited

Two Models of Time Constrained Target Travel Between Two Endpoints Constructed by the Application of Brownian Motion and a Random Tour

by

William Justin Comstock
Lieutenant, United States Navy
B.A., University of Michigan, 1972

Submitted in partial fullfillment of the
requirements for the degree of

MASTER OF SCIENCE IN OPERATIONS RESEARCH

from the

NAVAL POSTGRADUATE SCHOOL
March 1983

Author: W. Justin Comstock

Approved by: Donald P. Gaver
Thesis Advisor

Co-advisor

Chairman, Department of Operations Reasearch

Dean of Information and Policy Sciences

ABSTRACT

A target must choose a path between some origin and destination. The total travel time and the target speed are specified, and the target wishes to maximize the "randomness" of its track subject to the spatial and temporal constraints. Measures of effectiveness are developed against which the "randomness" of any path-producing method can reasonably be judged. Previous investigations into the scenario are reviewed and two models are developed, one using a random tour with drift and the other derived from Brownian motion. Statistics generated by Monte Carlo simulations for both models are compared. While the Brownian motion derived process is not always under perfect control of the constraints, if the timed arrival constraint may be slightly violated then that process performs better against the measures of effectiveness and is easier for a target to execute than is the random tour with drift.

TABLE OF CONTENTS

LIST OF TABLES

LIST OF FIGURES

ACKNOWLEDGEMENT

I owe much to Bob McDonough and John Sommerer of the Applied Physics Laboratory at Johns Hopkins. Bob arranged for me to visit the lab for six weeks and John, whose idea this thesis originally was, patiently followed my efforts and made suggestions which allowed me to proceed to the next hurdle on the course. I also thank Professors Donald Gaver and James Eagle of the Naval Postgraduate School. As my advisor, Prof. Gaver suggested and derived the Brownian bridge, as well as nudged me in the right direction when I veered from course. As co-advisor, Prof. Eagle read my thesis many times with great discrimination and suggested several significant improvements. Finally, I thank my wife Marie for showing endless patience and understanding while I thrashed my way through this project.

I. INTRODUCTION

This thesis will investigate two methods for constructing random target tracks between two specified endpoints. The target is constrained to begin its journey at one of the points and end it at the other after a stated elapsed time. Furthermore, either the mean target speed or the maximum and minimum speeds will be specified.

Consider the extreme case in which the distance between the two endpoints, the target maximum speed, and the specified elapsed time are such that the target is constrained to travel directly to its destination. Here there can be no randomness to the path, and an attacker needs very little target position information in order to make perfect predictions about future target position. Now imagine a less constrained situation in which there is considerably excess time. The target is able to travel around randomly during most of the period. It might choose to move quite randomly at the beginning, suddenly realizing at some critical point that it has just enough time remaining to travel directly to its destination. However, it is more intuitively sensible in this controlled time of arrival scenario to "spread" the randomness and effects of the constraints evenly across the time period.

The two scenarios above give insight about what characteristics of target travel are important. In the completely constrained case, the target's position does not vary at all from its expected position, resulting in an easily inferred position throughout the scenario. Furthermore, the target always points direcly toward its destination, as well as directly away from its origin. For a target that wishes to keep its origin and destination secret for some tactical reason, completely constrained travel is a giveaway. On the other hand, a target that travels about in an entirely random manner may never get to its destination.

It is clear that constrained target travel between two endpoints involves many tradeoffs among various constraints and choices. This thesis will develop a notion of "randomness" by devising measures of effectiveness that logically follow from the scenario and that also have strong intuitive appeal. Some previous approaches to the problem will be discussed briefly and then two new "recipes" for target travel will be developed in detail and evaluated against the measures of effectiveness adopted.

II. MEASURES OF EFFECTIVENESS

The previous scenario describing totally constrained target travel made apparent two dangers to the evasive target. First, the target risks divulging both its origin and destination because it always points toward its destination and away from its origin. It follows that the less constrained a target is, the less it necessarily points to destination and away from origin. Exactly how much course freedom is gained as the target becomes less constrained will be investigated in detail later. One might counter the importance of this pointing by claiming that, at best, the attacker obtains only a line of bearing to the origin or destination. While true, this argument neglects the possibility that other targets may pass the same way, with the same origin or destination. Sooner or later the attacker will get lines of bearing that cross with a regularity sufficient to specify the critical positions. Since origins and destinations might be important enough to be kept secret, one reasonable measure of effectiveness against which to evaluate any set of target paths is the absolute angle between the target's present course and the course from the target's position to its destination sampled at specified time intervals (c.f., Figure 1a). For the totally constrained target this angle will always be zero. In order

Figure 1:

Pictorial Representation of Two Measures of Effectiveness

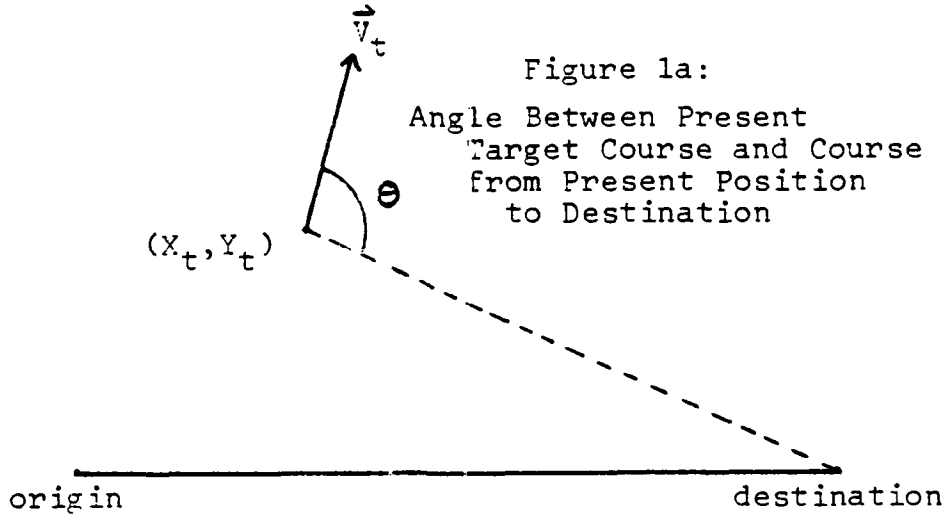

Figure 1a:

Angle Between Present Target Course and Course from Present Position to Destination

Figure 1b:

Radial Distance Between Present and Baseline Positions

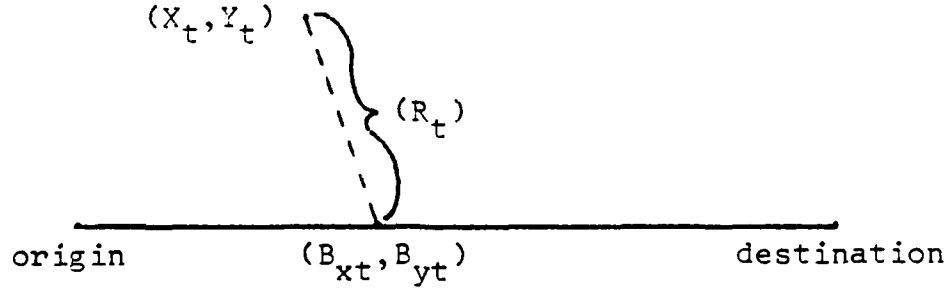

$$R_t^2 = (X_t - B_{xt})^2 + (Y_t - B_{yt})^2$$

to compare two different path generation procedures it will be helpful to produce a plot of this measure against time if, in fact, it is time dependent. Otherwise, it will be useful to calculate the mean pointing angle, its standard deviation, and perhaps an empirical density function.

The second undesirable quality of a completely constrained path is that the target's position always falls exactly on its baseline position, where baseline position (B_t) is defined as the point where the target would be at any time of its journey if it travelled directly to its destination at a constant speed. For example, if the distance between origin and destination is sixty distance units and the specified elapsed time for the problem is thirty time units, then the rate of travel along the baseline is two distance units per time unit. Ten time units after the start of the journey, the target's position is on the baseline twenty distance units from the origin and forty distance units from the destination. The baseline is important because the more constrained the target is, the closer it must stay on the average to the baseline. Increasing constraint on the target by decreasing allotted travel time or by increasing baseline length straightens out the target path with the result that inferred positions are easier to obtain. Very importantly, even if the target is not forced to stay near the baseline as a result of being constrained, but chooses to do so by hovering or zig-zagging along the

line, an inferred course and position are easily obtained. Even worse, such an inferred course will most likely point to the destination or from the origin. Accordingly, the second measure of effectiveness shall be the mean square radial distance between the present target position and the baseline target position at specified time intervals during a journey (c.f., Figure 1b). This statistic will be denoted as $E[R_t^2]$. The squared radial distance has been chosen rather than the radial distance because previous investigations into the problem, which will be cited in the next chapter, have tended to use radial distance squared. It is easier to handle analytically than is R_t, and can be viewed as the sum of the x and y component squared distances from the component baseline positions at any time t:

$$R_t^2 = (X_t - \beta_{xt})^2 + (Y_t - \beta_{yt})^2 \qquad (1)$$

It would be not difficult to integrate R_t^2 over the whole time interval for an individual path in order to get a scalar value for this performance measure. Likewise, the mean square radial distance ($E[R_t^2]$) could be integrated for each particular path-producing recipe in order to obtain a scalar measure for that method. Then, two different path methods might be compared and, all other measures being equal, the method with the highest value selected. However, the reduction of this measure of effectiveness to one scalar

can result in great loss of information. Two path generation procedures might have the same value by the scalar measure, but be characteristically different. One might tend to have relatively large values of $E[R_t^2]$ near the origin and destination, while the other method might have small values there, with large values for t in the middle of the travel period. Furthermore, each of these two different path recipes might be more desirable than the other under different circumstances. For instance, if it is not important to keep secret the origin and destination because they are already known to the enemy, but it is important to be as undetectable as possible (or if detected, as difficult as possible to redect) in between origin and destination, then the target would probably prefer the latter of the two path-producing methods. In any case, for any path-producing recipe, the captain of the target should be able to look at the plot of $E[R_t^2]$ as function of time. Thus, the measure of effectiveness itself shall be either a plot of $E[R_t^2]$ against time, the function that describes it as such, or a list of ordered pairs with time as the first element and mean square radial distance as the second.

A careful observer might object to this measure of effectiveness. While it is true that a highly constrained target will exhibit a small $E[R_t^2]$ for all t and have easily inferred positions, this does not necessarily mean that a large $E[R_t^2]$ will guarantee that target position will be

difficult to infer. In fact, if maximizing $E[R_t^2]$ over the entire time period is taken as the only measure of effectiveness, it should be almost as easy to infer future position from a few past positions as it is in the totally constrained case. Imagine a baseline ten distance units long, a maximum target speed of four distance units per time unit (4 d/t) and a specified travel time of four time units. It seems sensible that the target would travel at maximum speed the entire time in order stay as far away from its expected position as possible. For a good analogy, imagine a stick ten distance units long with a piece of string sixteen distance units long attached to it, each end to each end. Then, the target might choose a track to maximze the area between the stick and the string. (The analogy is not perfect however; in the stick and the string example the radial distance (R_t) integrated over the entire time period is being maximized rather than the radial distance squared (R_t^2). One possible path choice is to drive the target straight away from the baseline at about a fifty degree angle for eight distance units, then turn back and go directly to destination. The area of the isosceles triangle thus formed with the stick as the base is approximately 31 distance units squared. But a clever hard working target could drive in a circular arc, thus enclosing approximately 39 distance units squared. This path, while producing a large $E[R_t^2]$ at each time t, is not very "random" and might be easily targeted.

The third and final measure of effectiveness is important in at least two ways. The first pertains directly to the shortcoming of the second measure of effectiveness taken by itself. Given a certain recipe for producing paths, it is necessary to produce many of them in order to obtain statistical estimations of both of the two measures of effectiveness already chosen. It may be possible to apply some non-linear regression method to any path, and to extract an estimate of future position to use as the expected position for any time t, rather than use baseline position as already defined. Such a method would quickly identify the smooth curves produced by any path recipe which maximized the mean square radial distance only. But the task would be quite difficult and costly, especially when applied to the several hundred paths necessary to produce good statistics. In order to save effort and money, the third measure of effectiveness will subjectively judge how representative paths from each generating method "look". Against this measure, any path which maximizes $E[R_t^2]$ alone will be rejected at a glance if it exhibits long straight legs or a predictably curved path. However, if a path does not look so regular as to be predictable, then a large $E[R_t^2]$ is desirable because it means the target is staying away from the critical line between origin and destination.

A second very important reason that paths will be visually inspected is that they must be able to be executed

by an actual target. Hence, an experienced person must judge whether or not a path is practical regardless of its statistics. For example, a high-curvature path which maximizes $E[R_t^2]$ may not be implementable.

There are, then, three measures of effectiveness that shall be used to judge path-producing recipes. Though they were introduced in a different order to facilitate logical development of them, they will be applied to a path procedure as follows. First, a representative path must "look good" by being practical, executable, and random looking (no noticeable regularities). If a path can pass this first important test, then several hundred will be generated using the same procedure, and the mean angle (and its standard deviation) between present course and course from present position to destination will be calculated at specified time intervals. Then, the mean square radial distance between present position and baseline position will be calculated at each specified time interval. The $E[R_t^2]$ will thus be estimated at various stages of path completion. If two path generating recipes both produce paths that meet the origin, destination, time, and speed constraints, and "look good" by the first measure of effectiveness, then the path which exhibits the least pointing to destination as judged by the second measure of effectiveness and the greatest $E[R_t^2]$ at a given stage of path completion shall be judged to be the more desirable path. Some comparisons will no doubt result in a

situation in which both procedures produce paths which "look good", but each of the two methods has a better evaluation than the other in one of the other two measures. One might try to form some weighted combination of the two measures, but this is dangerous because measures of effectiveness do not combine well; at minimum, their units are not generally on the same interval scales. Such reductionism is not necessary anyway. One need only regard both of the last two measures and decide when it is advantageous to weight one subjectively over the other. In fact, any formal weighting system would probably not be able to capture all scenario dependencies as well as a subjective weighting.

III. PREVIOUS INVESTIGATIONS

While several approaches to the problem of randomizing target motion are possible, one of the most appealing is investigated in detail by Washburn [Ref. 1]. In his model a target takes a random tour by choosing its direction of travel from a uniform (0,2π) probability distribution and its length of travel on the selected heading from an exponential distribution with parameter λ (mean number of turns per time unit). Thus, turning points are the jumps of a Poisson process with parameter λ, and at any point during the process both the backward and forward recurrence times are themselves distributed exponentially with parameter λ. This property of "memorylessness" is very appealing. The probability that the target does not turn by time (t+a), given that it has not turned by time t is the same as the probability that the target will not turn during the time interval (0,a). In other words, in deciding at any point in time when to turn in the future, the target does not remember how long it has already traveled on the same course. Hence, an attacker may not infer either that the target will stay on a new course if it just turned to it, or that the target will turn soon because it has been on the same course for a long time. Because of the desirability of giving an attacker so little information, each leg of target travel is chosen by draws

from the following distributions:

$$f(\theta) = \begin{cases} 1/2\pi & 0 \leq \theta \leq 2\pi \\ 0 & \text{otherwise;} \end{cases}$$

$$f(t) = \begin{cases} \lambda e^{-\lambda t} & t > 0 \\ 0 & \text{otherwise.} \end{cases} \qquad (2)$$

After much mathematical manipulation, Washburn derives the probabilty density of the target's radial distance from its origin, given no initial course information, to be:

$$f(r,t)=[1/2\pi(Vt)^2][\lambda t/(1-r^2)^{1/2}]\exp[-\lambda t(1-(1-r^2)^{1/2})]. \qquad (3)$$

He also makes some interesting observations:

1. The larger λ is the more the distribution piles up around the origin.
2. Given no turns, the target is uniformly distributed on a circle of radius Vt (throughout this thesis, a 'V' will denote a scalar which is the magnitude of the vector denoted by '$\vec{V}$').
3. Very remarkably, given that two steps have been completed at time t, the target is uniformly distributed in the circle of radius Vt, not including the circumference.

The first two observations go hand in hand. Recall from Chapter I that a target which hovers about the baseline or

zig-zags along it has a small $E[R_t^2]$ since it is rarely far from its baseline position. Washburn's distribution quantifies exactly how much the target remains near its expected position relative to how much the target "hovers", as indicated by the parameter lambda. The only difference is that Washburn's model has no drift, resulting in the expected position being a single point rather than a baseline of many points as in the drift case. A turning parameter of lambda equal to infinity creates the degenerate case in which the target is distributed on top of its origin with probability equal to one. The other degenerate case occurs in observation two when the target does not turn and is then necessarily on the circle of radius Vt. Just as noted in Chapter I, $E[R_t^2]$ may be high in this form of degeneracy, but given any two bits of position information, future position can be inferred perfectly because the target has been travelling in a straight line.

Though it is interesting that the target is uniformly distributed on the disk of radius Vt if it just happens to have finished leg two by time t, this fact really does not help a target evade an attacker. Given the set of instructions by which paths are generated, it would be purely coincidental that the second leg is completed right when the attacker looked for the target (the probability is zero). One might say that the target should plan to finish the second leg just when the attacker is expected. For example,

the target might know when it conducts some type of evolution that makes itself more detectable. Also, it also might know from how far away the attacker must come and at what speed, so it has a good idea when its window of vulnerability is. But if it uses this information to plan two legs then it is not following a random tour as prescribed by the probability distributions set forth. If the target is going to break the rules, it may as well just pick a point at random inside the circle of radius Vt and head for it. This procedure will guarantee that the target has sampled uniformly over the disk.

Belkin [Ref. 2] does pioneering work in comparing Washburn's random tour process with a Gauss-Markov process for describing diffusion, the Ornstein-Uhlenbeck (IOU) process. As a result, Belkin finds that the mean square radial distance of a target from its expected position at time t in a random tour process is:

$$E[R_t^2] = 2(V^2/\lambda^2)\ (e^{-\lambda t} + \lambda t - 1). \qquad (4)$$

Belkin [Ref. 3] further embellishes his analytic work on the random tour process by deriving the mean square radial distance for a random tour with arbitrary course change distribution to be:

$$E[R_t^2] = 2(V_w^2/\lambda^2)\ (1 - \mu_x^2 - \mu_y^2)\ (e^{-\lambda t} + \lambda t - 1), \qquad (5)$$

where,

$$\mu_x = \int_0^{2\pi} \cos\theta \, dF(\theta)$$

$$\mu_y = \int_0^{2\pi} \sin\theta \, dF(\theta). \qquad (6)$$

Here $F(\theta)$ is the cumulative distribution function of θ for which there may or may or not be a proper density function. The subscript w on V_w indicates that the velocity is total velocity through the water, comprised of both a drift component and a randomizing component which will be explained later. Notice that for the uniform distribution of the Washburn's random tour model, $\mu_x = \mu_y = 0$, and equation (3) results as expected.

The notion of an arbitrary course change distribution is important because the expected position of the pure random tour process is the origin at time zero. As such, the process will never cause a target to migrate toward its destination. Therefore, it is necessary to introduce some bias into the selection of the courses in order to keep the target moving in the correct direction toward its destination; and even a course distribution alone will not cause a target to visit the destination without the addition of some further constraining process. While an infinite

number of arbitrary course selection distributions are possible, several look promising when applied to the present problem. Loane [Ref. 4] suggests:

$$f(\theta) = 1/2\pi\,(1 + \alpha\cos\theta) \qquad \text{for } \theta \in (0,2\pi),\ \alpha \in (0,1), \tag{7}$$

where bias in the positive x direction can be controlled by the selection of the parameter α. Because constraining target travel by course distribution alone only causes the target to migrate toward its destination, without giving any guarantee that the endpoint will be visited, some process must be devised to meet the visitation constraint. One of many possible course distributions, which also injects the time constraint into course selection, is:

$$\theta \sim \text{normal}\,[\text{CUS}, \text{Arcos}(T_d/T_r)] \tag{8}$$

where CUS is the course to the destination at the beginning of the leg, T_d is the time it would take to go directly to the destination at mean speed or maximum speed (whichever is selected as important for a particular run), and T_r is the time remaining in the problem. Notice that in the most constrained case in which $T_d = T_r$, the variance of the course distribution equals zero and the target travels straight to its destination. While this course distribution causes the target to travel over the destination, it does not control when it will cross it. Hence, it does not solve the

controlled time of arrival scenario devised in Chapter I. Belkin [Ref. 5] meets the visitation constraint with the IOU process and is able to distribute the contraints evenly across the whole path through optimal control of velocity. This means that the target arrives at destination when it has to, without either traveling to it straightaway and hovering for the remainder of the period, or by randomizing travel until the last possible opportunity to get straight to the destination on time. Nonetheless, mean square radial distance from baseline position will necessarily need to begin decreasing at some point in order to guarantee that the target visits its destination. Two observations made by Belkin motivate the approaches taken in this thesis for devising path recipes. He states [Ref. 6] that "...it is possible to approximate a random tour process with arbitrary course change distribution by an IOU process with linear drift." He also notes [Ref. 7] that "...as the constrained process approaches the terminal constraint at T, the process behaves precisely like an unconstrained process running backwards in time from T." T, in this instance, is the total time alloted for the problem and the terminal constraint is the requirement for the target to be at the destination at T.

As a result of Belkin's insights, the first of two path producing recipes that will be developed in this thesis will treat constrained travel between two endpoints as a random tour process with drift (distance between endpoints divided

by total time), executed from both endpoints with an attempt to connect the two separate paths somewhere in the middle. The drift vector applied to the path beginning at the origin will "blow" the target toward the destination, while the drift for the path starting at the destination will "blow" in the opposite direction, toward the origin. This approach constitutes a discrete approximation of the IOU process with drift, wherein the random tour out of the destination is one half of the total problem run in reverse.

Belkin's solution to the problem of constrained target travel is the IOU process and he has developed a computer simulation named IOUTRK for which he presents some sample paths [Ref. 8]. While the genesis leading to his adoption of the IOU process begins with Washburn's random tour, Belkin proceeds to attempt an approximation of the random tour process using Brownian diffusion [Refs. 9,10]. However, his investigations lead him [Ref. 11] to the very clever realization that the functional form of the mean square radial distance, $E[R_t^2]$, is exactly the same for the IOU process as for the random tour after making only two simple parameter substitutions [Ref. 12]. He concludes his analysis [Ref. 13] by stating that "...if one is constrained for theoretical or computational reasons to approximate the motion of a randomly touring target by Gaussian diffusion, then the Ornstein-Uhlenbeck displacement model is to be preferred to the Brownian motion model."

The random tour process is important and has many desirable properties that will be discussed further when the first new path recipe in this thesis is developed and analyzed. As indicated previously, the random tour will not be approximated by any other process; it will itself be executed in a new way. The second model to be offered in this thesis will examine Brownian motion, not as an approximation of a random tour, but as a basis for solving the constrained target motion problem in another way. Though rejected by Belkin as an approximation of the random tour process, Brownian motion stands alone as a method for solving the problem at hand in a very novel way.

IV. PROCEDURE

A. RANDOM TOUR WITH DRIFT

In order to evaluate the random tour with drift against the measures of effectiveness delineated in Chapter II, a Monte Carlo simulation is devised. Specifically, two random tour processes are executed, one from each endpoint, in order to guarantee that the destination (actually the starting point of the second process) is visited as required by the constraints. Recall from Chapter III that the reason for executing two separate processes stems from Belkin's observation that the path approaching the destination looks like an unconstrained random tour run in reverse. Hence, the path which visits the destination is constructed by executing an unconstrained random tour originating at the destination. For all paths, and without loss of generality, the origin is zero on the x axis of a Cartesian coordinate system in two-space and the destination is however many distance units desired in the positive x direction. The random tour beginning at the origin is "blown" in the positive x direction by the drift vector and the process originating at the destination is "blown" in the negative x direction by an opposing drift vector of the same magnitude. The goal is to generate two paths that "blow" into each other somewhere between origin and destination. At the outset, the distance

between origin and destination, the time period, the mean target speed through the water (V_w), and the target turning rate (lambda) must all be specified. Drift velocity is then in the positive or negative x direction, depending on which of the two random tours is being executed, with a magnitude equal to total baseline distance divided by total problem time. Figure 2 below illustrates the other important velocity, the randomizing velocity $\vec{V}_r$, the magnitude of which must be computed before the random tour can begin.

Figure 2:

Water Velocity as a Composition of Drift and Randomizing Velocities

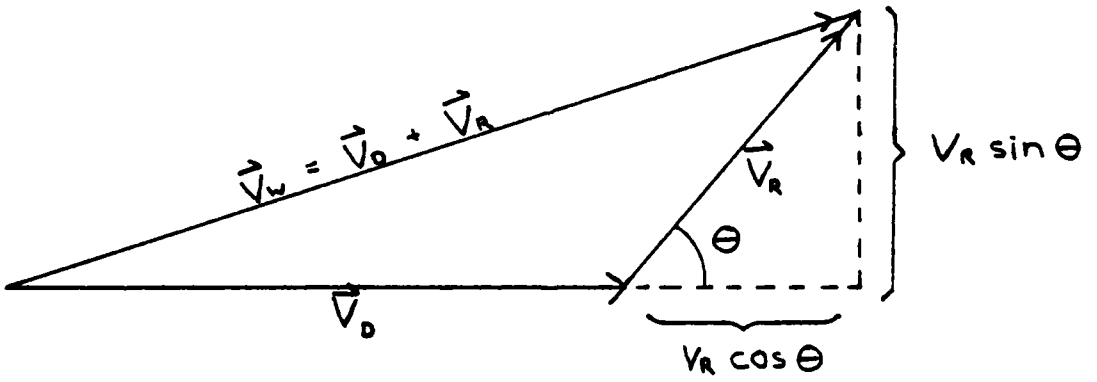

Because the target must have a mean speed through the water of V_w, and V_{drift} is determined by baseline length and total run time, there is no freedom in choosing mean V_r. Recall that the angle theta is the direction of target travel chosen from the uniform probabilty distribution (0,2π) and notice in Figure 2 that $\vec{V}_w = \vec{V}_d + \vec{V}_r$.

Then:

$$E[V_w^2] = E[|\vec{V}_d+\vec{V}_r|^2] = \int_0^{2\pi} 1/2\pi[V_r^2\sin^2\theta+(V_r\cos\theta+V_d)^2]$$

$$= 1/2\pi \int_0^{2\pi} (V_r^2 + V_d^2 + 2V_rV_d\cos\theta)\ d\theta \qquad (9)$$

$$= V_r^2 + V_d^2$$

Hence, given V_d and a desired mean V_w, the randomizing velocity for the random tour with drift should be:

$$V_r = (V_w^2 - V_d^2)^{1/2} \qquad (10)$$

Notice that as the drift speed approaches the water speed, the randomizing speed goes to zero. This is reasonable because when the target has just enough time at a given speed to go straight to the destination, all its velocity goes toward matching the drift velocity and there is no excess velocity left over for any randomization; the target is totally constrained.

With these preliminaries taken care of, the simulation is executed beginning with the "left" path (out of the origin at zero on the x axis) according to the following procedure:

1. Choose the direction of travel from U(0,2π).

2. Select the length of each leg of the process as $V_r t$, where t is determined by a draw from an exponential distribution with parmeter lambda.
3. Compute the actual vector $\vec{V}_w$ describing travel for the leg by adding a prorated drift vector $\vec{V}_d$, the magnitude of which equals [(t / total problem time) x baseline length], to $\vec{V}_r$ which was determined in steps 1 and 2.
4. Continue executing steps 1-3 until the cumulative travel time for all left side legs is at least .475 of the total time for the whole problem.

After one left side path is simulated, a similar process is executed from the "right" side (destination) using an opposite drift direction. As a result there are now two random tour paths which migrate toward each other at the determined drift rate. The two processes use up at least .95 of the total time alloted for the target travel from left to right. Now, a circle with radius .05 x total time x desired water speed is drawn around the left endpoint. The proportion of time left in which to join the two sides is not arbtrary, but depends on the length of the total time of the problem. Here, the total time is assumed to be between 30 and 60 time units, making the joining period between 3 and 6 time units. During this connecting period the target should maneuver as suggested by λ, laying down a path that will make the connection. If the right path endpoint falls within the

circle, then a "match" has occurred and the two connected paths constitute a complete sample path satisfying all constraints. If a match is not realized in a specified number of iterations of the right path, then a new left path is executed and another attempt to generate a matching right path is made. The number of right paths that are generated in attempting to match a given left path and the number of left paths that are generated after a right path match iteration limit is reached can both be controlled by parameters in the simulation. The entire process is continued until 100 matches (or any other number desired) are obtained or until the limits for the number of attempts are reached. The motivation for this procedure of matching is twofold. First, desired statistics can be generated to test the symmetry of both sides since many right side and left side paths will be generated during the quest for 100 matches. Secondly, in attempting to get matches, the number of right sides allowed in order to match a given left side can be strictly controlled. The lower the limit on right sides, the more likely it will be necessary to generate another left side. In this manner, the total number of left sides generated in order to obtain 100 matches can be much greater than 100, and the number of right sides will be even greater yet since right sides are constrained to match left sides and not vice versa. This path generating method results in two complete distributions of paths for the left side. Some left hand

paths result in matching right hand paths, while other left paths are rejected because no right paths can be generated (within limits) to match them. The retained left paths comprise a set which will be called the "clipped" set, while all paths, rejected or not, will be called the "unclipped" set. These names are reasonable because the paths that match are more constrained; they have not been rejected as unacceptable. A comparison of the statistics of interest for both left hand sets will indicate how much degradation results from constraining the clipped set. Additionally, there is a third set of paths which contains all the right paths which match left paths. Statistics are generated for this set in order to check symmetry with the left hand clipped set.

In order to facilitate the generation of valid statistics it is necessary to sample the left and right paths at the same specific time intervals. While it is much easier to sample a path at the end of each leg, the resulting statistics do not provide consistent comparisons along the time line. Accordingly, statistics are generated at times determined as a function of the turning rate, λ, so that the probability of generating statistics twice on the same leg is .001. The statistics generated at each time check for all three sets of paths are:

1. Mean magnitude of the angle between present course and

course to destination from present position; variance and standard deviation of that mean angle.

2. Mean square radial distance between baseline position (pure drift prorated for cumulative run time) and actual position.

Using the procedure described here, statistics are generated for a water speed of 4.0 dist/time and drift rates of 3.75, 3.0, 2.0, 1.0 dist/time, all for turn rates of 1.0, 2.0, and 4.0 per time unit. There are a total of twelve cases.

B. BROWNIAN-DERIVED MOTION

Since Robert Brown first observed the highly irregular motion of suspended pollen particles in 1827, mathematicians and scientists have spent a great amount of time and effort investigating Brownian motion, and its widespread applicability to naturally occurring events makes it a reasonable candidate for randomizing target motion. From a probabalistic viewpoint Freedman [Ref. 14] defines normalized Brownian motion to be a stochastic process $(B(t):0 \leq t < \infty)$ on a sample space Ω with properties (a-c) for points $\omega \in \Omega$:

(a) $B(0,\omega) = 0$ for each ω,

(b) $B(.,\omega)$ is continuous for each ω,

(c) for $0 < t_1 < t_2 <...< t_{n-1} < t_n$, the increments $B(t_1)$, $B(t_2) - B(t_1),..., B(t_n) - B(t_{n-1})$ are independent and

normally distributed, with means 0 and variances t_1, $t_2 - t_1, \ldots, t_n - t_{n-1}$.

Additionally, this process is Markovian, meaning that the future is conditionally independent of the past, given the present;

$$\begin{aligned} &= P(X_{t+1} \leq i_{t+1} \mid X_0 = i_0, \ldots, X_t = i_t) \\ &= P(X_{t+1} \leq i_{t+1} \mid X_t = i_t) \end{aligned} \tag{11}$$

where the i's are elements of the state space for the random variable X.

Once again, the problem of constrained target motion shall be framed in two-space using a standard Cartesian coordinate system. Taking position to be specified by each component separately, the conditional probabilities for each coordinate at time t, given the initial constraints are:

$$\begin{aligned} &P(X(t) = x \mid X(0) = 0, X(T) = L) \\ &P(Y(t) = y \mid Y(0) = 0, Y(T) = 0) \end{aligned} \tag{12}$$

where t is cumulative run time, T is total alloted time and $(0 \leq t \leq T)$, L is the positive x coordinate of the destination, and 0 is the y coordinate of destination. Hence, the Cartesian layout is exactly as it is for the random tour case. Conditioning the Brownian motion constructs a "Brownian bridge" between the origin and the destination, by which the initial problem constraints are met. The x component conditional probability expands to:

$$\frac{P\,(\,X(t) = x \mid X(0) = 0\,)\;.\;P\,(\,X(T) = L \mid X(t) = x\,)}{P\,(\,X(T) = L \mid X(0) = 0\,)}$$

$$= \frac{P\,(\,X(t) = x,\, X(T) = L \mid X(0) = 0\,)}{P\,(\,X(T) = L \mid X(0) = 0\,)} \qquad (13)$$

and the conditional density when X(t) is distributed Gaussian becomes:

$$\frac{\dfrac{\exp(-1/2[(x-0)/(\sigma t^{1/2})]^2)}{(2\pi)^{1/2}\,.\,\sigma\,.\,t^{1/2}} \;.\; \dfrac{\exp(-1/2[(L-x)/(\sigma(T-t)^{1/2})]^2)}{(2\pi)^{1/2}\,.\,\sigma\,.\,(T-t)^{1/2}}}{\dfrac{\exp(-1/2[(L-0)/(\sigma t^{1/2})]^2)}{(2\pi)^{1/2}\,.\,\sigma\,.\,T^{1/2}}} \qquad (14)$$

$$= \frac{\exp(-1/2\;Q)\;.\;T^{1/2}}{(2\pi)^{1/2}\,.\,t^{1/2}\,.\,(T-t)^{1/2}}$$

where:

$$Q = (x^2/\sigma^2) + ((L-x)^2/[\sigma^2(T-t)]) - (L^2/\sigma^2 T)\,.$$

After completing the square for Q and simplifying, the conditional density reduces to:

$$\frac{\exp(-1/2[(x-Lt/t)/(\sigma^2 t(1-t/T))]^2)}{(2\pi)^{1/2}\,.\,\sigma\,.\,(t[1-(t/T)])^{1/2}.} \qquad (15)$$

Hence, X(t) and Y(t) [by a similar derivation] are distributed:

$$X(t) \sim \text{Normal}\;[\;Lt/T,\; \sigma^2 t(1 - t/T)]$$
$$Y(t) \sim \text{Normal}\;[\;0,\; \sigma^2 t(1 - t/T)]. \qquad (16)$$

In both distributions σ^2 is a physical parameter that may be specified, and the total variance describes a parabola when plotted against t. The maximum variance is $(\sigma^2)(T/4)$ and occurs at $t = T/2$. Very importantly, the variance is zero at both the origin ($t = 0$) and the destination ($t = T$).

One of the measures of effectiveness chosen in this thesis against which to judge a target path examines how a path "looks" and whether it is executable by a crew. Brownian motion, as defined, is not executable because it is a continuous process with an everchanging velocity, and as such, is impossible for a large target to duplicate. However, there is no reason why the continuous process cannot be sampled at various times and the selected points be made the endpoints for legs of straight line travel. Of course, as the time interval between samples is lengthened, the linear approximation connecting the sample points becomes less "Brownian". Nonetheless, the process still retains vestiges of its Gaussian properties, and the flavor of Brownian motion.

An exponential distribution should be used to determine the sample times for the same reason that is advanced for the random tour: the memoryless property applied to course change is advantageous to the target. Exactly how to sample from the normal distributions (16) is the last problem to be solved before a procedure can be devised for executing paths.

One might sample by generating a string of exponential

random variables using the desired parameter lambda in order to get the time jumps (t_1, t_2,..., t_n) of the Poisson process which determines course change; then make a draw from each from the x and y normal distributions at times t = t_1, $t_1 + t_2$,..., $t_{n-1} + t_n$ to obtain x and y coordinates for the path legs. While the mean of the y coordinate draw is always zero, there is nothing in this method to prevent one y coordinate draw from falling on one side of the x axis and the next draw on the other side. As the cumulative time approachs T/2 the variance of the draw becomes relatively large and it is quite likely that two consecutive draws which fall on opposite sides of the mean will be very far apart relative to the corresponding time step. A similar argument applies to the x coordinate, and because position is determined by both coordinates, if two consecutive draws are on the opposite sides of their means for both the x and y coordinates, the distance between two consecutive positions could be very far apart. The result is that a ridiculously high velocity is required in order for the target to travel from one sample point to its successor in the given time step. What is needed is some way to guarantee that a successive position is tied to the one before it. Future position must be conditioned on present position, and that is what is missing in this method. One possible remedy might be to reflect each draw across its mean if needed. Thus, the variance of the draw is preserved while the distance between

successive positions is shortened to a manageable length. However, this type of optional reflection does not capture the true Markovian property of each draw, but it does provide insight into how each successive draw should be done.

Suppose that the first draw is carried out without reflection as described above. The first leg will connect the origin with a point selected by a draw from the two normal distributions (16) substituting $t = t_1$ (the first time selected from the exponential distribution). Invoking the Markovian property, all information prior to this latest point is superfluous. Hence, there exists a completely new controlled time of arrival problem, wherein the latest point becomes the new origin and the line between that point and the destination becomes the new baseline. The total run time for the new problem is $T - t_1$. This iterative process continues until the original total time (T) has expired. On the final leg, the cumulative time for the two coordinate draws is $t = t_1 + t_2 + \ldots + t_n = T$, so that the variance in (16) goes to zero and the target visits its destination on time. This procedure is a sensible one that seems to capture the properties of Brownian motion while at the same time producing discrete linear legs of target travel. Thus, it is the procedure adopted to produce the second type of path developed in this thesis, and the steps of the recipe are:

1. Select baseline length (distance between origin and

destination = L), total run time (T), turning rate (λ), maximum and minimum target speed, and physical parameter for variance (σ^2). Simulation frame of reference is a Cartesian coordinate system in 2-space, with origin at (0,0) and destination at (L,0).

2. Generate a string of random variables from an exponential distribution with parameter lambda, and truncate the nth value in the string so that the sum of the random variables $t_1 + t_2 + \ldots + t_n = T$.
3. Make a draw from the normal distributions in (16), using t = cumulative run time. For the first draw, $t = t_1$; for the second draw, $t = t_1 + t_2$; and so on.
4. Measure distance between new point (X_i, Y_i) and previous point (X_{i-1}, Y_{i-1}). If the distance/t_i is greater than the maximum target speed, truncate the leg as illustrated in Figure 3 if the distance/t_i is less than the minimum target speed, extend the leg. Either truncation or extention results in new (X_i, Y_i).
5. Reframe problem as a completely new one, using (X_i, Y_i) as the origin, (L,0) as the destination, and T = time remaining. Execute steps 3,4 again. The last draw forces (X,Y) to be equal to (L,0) unless truncation or extention occurs, in which case problem ends on time with target short of destination, or target continues to destination, in which case total travel time exceeds T. One path is completed.

Figure 3:
Leg Truncation and Extension

Figure 3a: Truncation

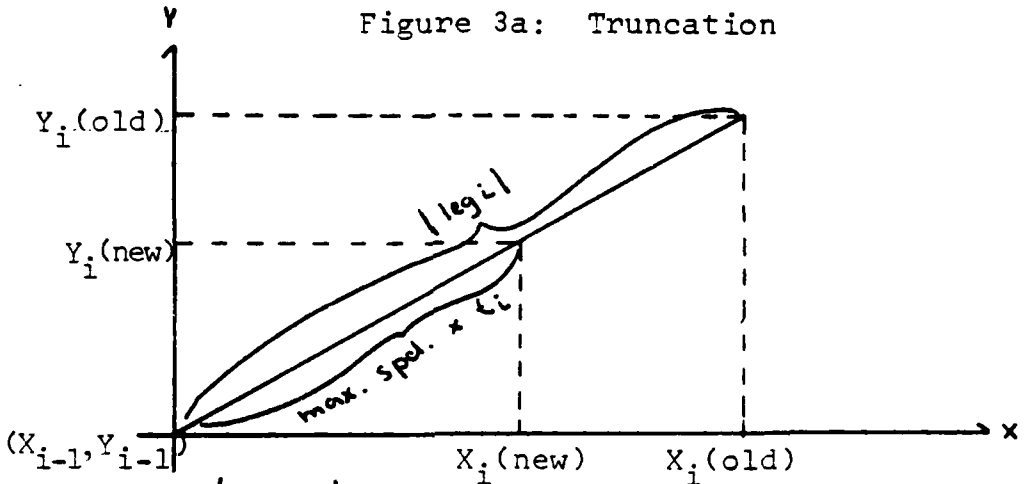

$|\text{leg } i| > \text{max. spd. x } t_i$;

so $|\text{leg } i \text{ (new)}| = \text{max. spd. x } t_i$

Figure 3b: Extension

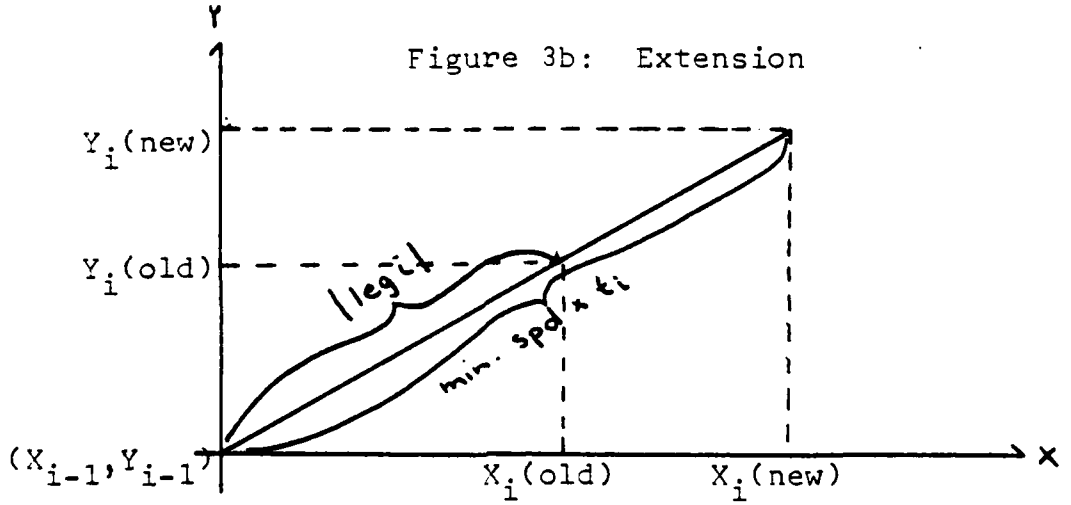

$|\text{leg } i| < \text{min. spd. x } t_i$;

so $|\text{leg } i \text{ (new)}| = \text{min. spd. x } t_i$

6. Generate several hundred such paths and compute the statistics of interest for each one at specific time intervals (mean square radial distance between present position and baseline position of original problem; and absolute difference between target present course and course to destination from present position). Look at plots of paths to determine if they "look good", as discussed in Chapter II.

After statistics and plots are generated for both the random tour and Brownian motion derived paths, the task is to compare the two approaches in order to determine their respective strengths and weaknesses.

V. RESULTS

A. RANDOM TOUR WITH DRIFT

One measure of effectiveness for judging paths requires that they "look good", as detailed in Chapter II. It makes sense to try this measure on a path procedure first before expending effort to evaluate a mass of statistics. If the candidate paths can be rejected on sight then time will not be wasted on the other two measures.

Figures 4a-f are representative paths generated by the random tour with drift method. The circle in these figures, as described earlier, is inscribed with the end of the left path as its center and has a radius = V_w x time remaining in problem after the execution of both the left and right paths. Thus, the target can easily travel from the end of the left leg to the end of the right leg in the allotted time at the stated water speed. The ratio V_d/V_r listed on each of the figures measures just how constrained each path is. The ratio ranges from zero for the unconstrained case (random tour without drift) to positive infinity for the totally constrained case (straight line between origin and destination). Figure 4a shows a path for which $V_d/V_r = 2.69$; clearly this path does not "look good" and is not acceptable. It is almost a straight line between origin and destination, and future target position is easily inferred from only a few

Figure 4a: Random Tour With Drift

$V_d/V_r = 2.69$

$\lambda = 2.0$

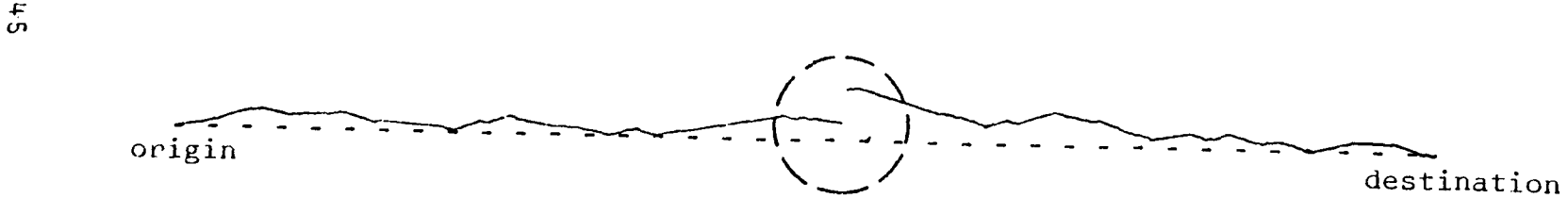

Figure 4b: Random Tour With Drift

$V_d/V_r = 1.13$

$\lambda = 2.0$

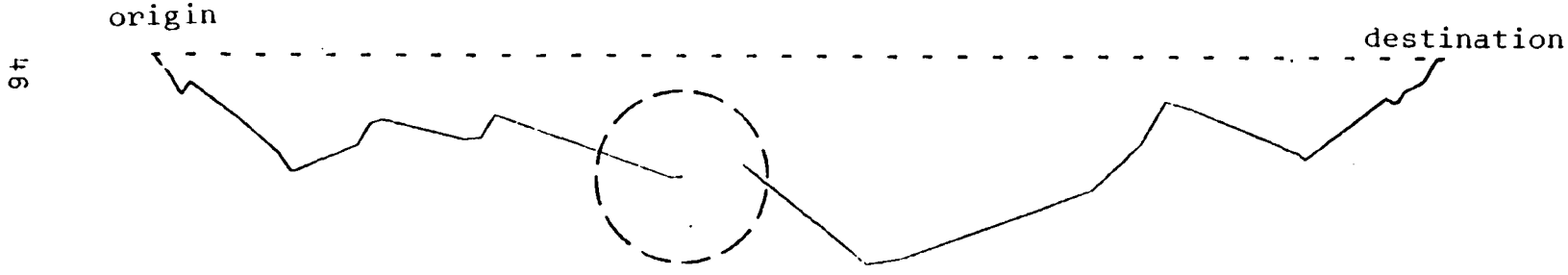

Figure 4c: Random Tour With Drift

$V_d/V_r = 0.58$

$\lambda = 2.0$

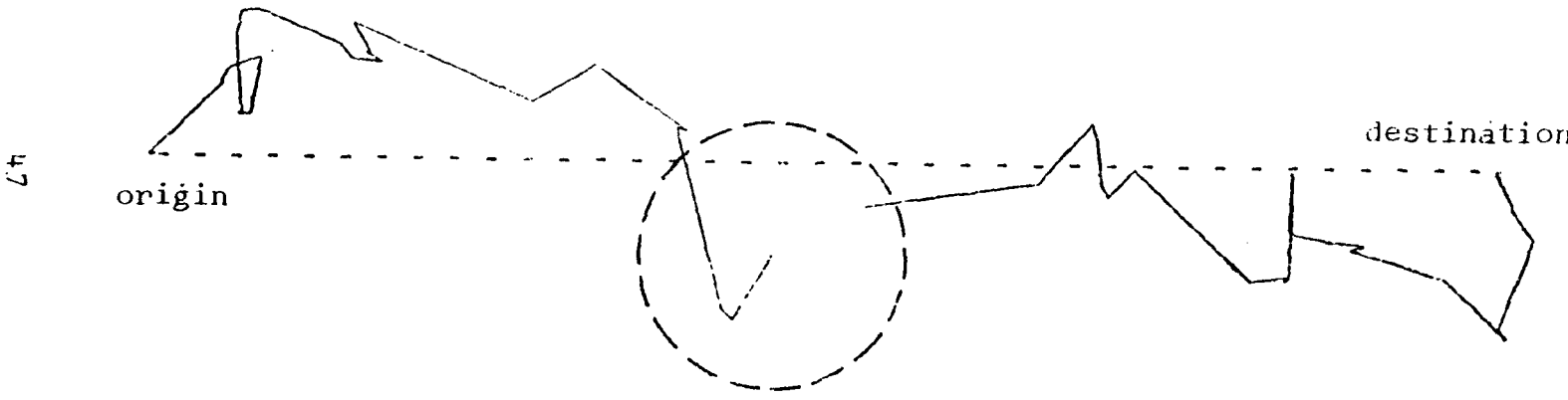

Figure 4d: Random Tour With Drift

$V_d/V_r = 0.26$

$\lambda = 1.0$

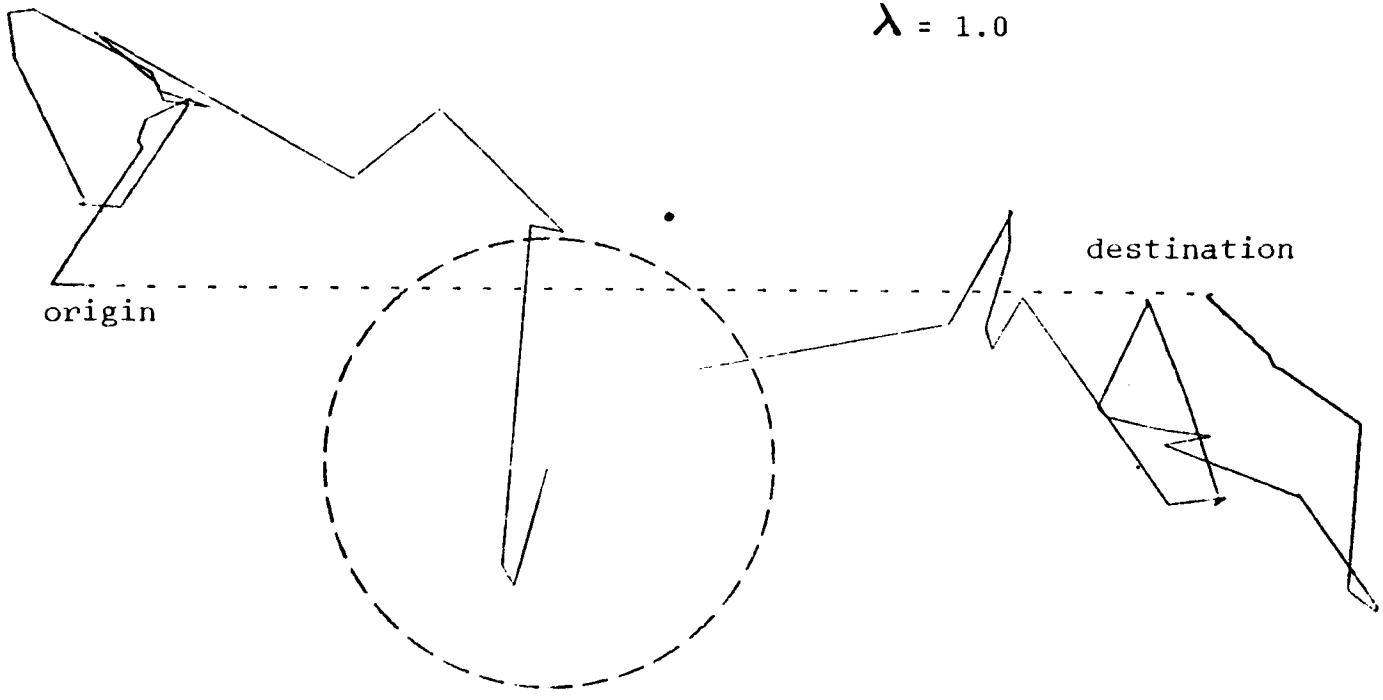

Figure 4e: Random Tour With Drift

$V_d/V_r = 0.26$

$\lambda = 2.0$

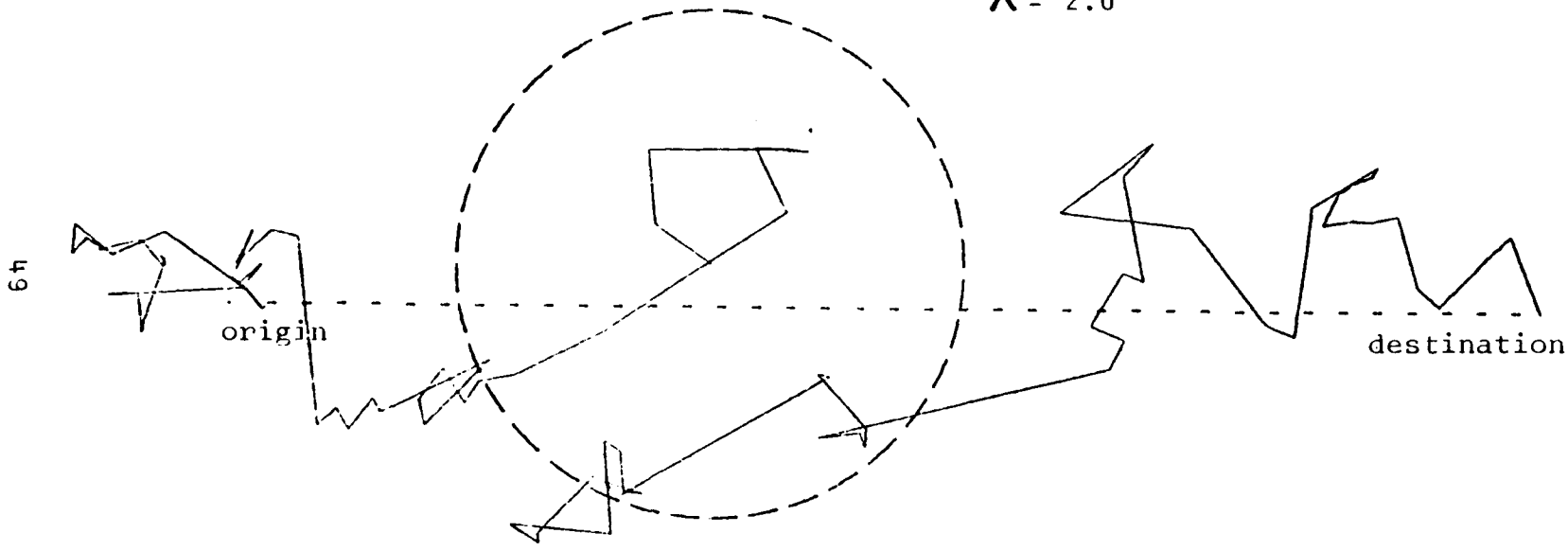

Figure 4f: Random Tour With Drift

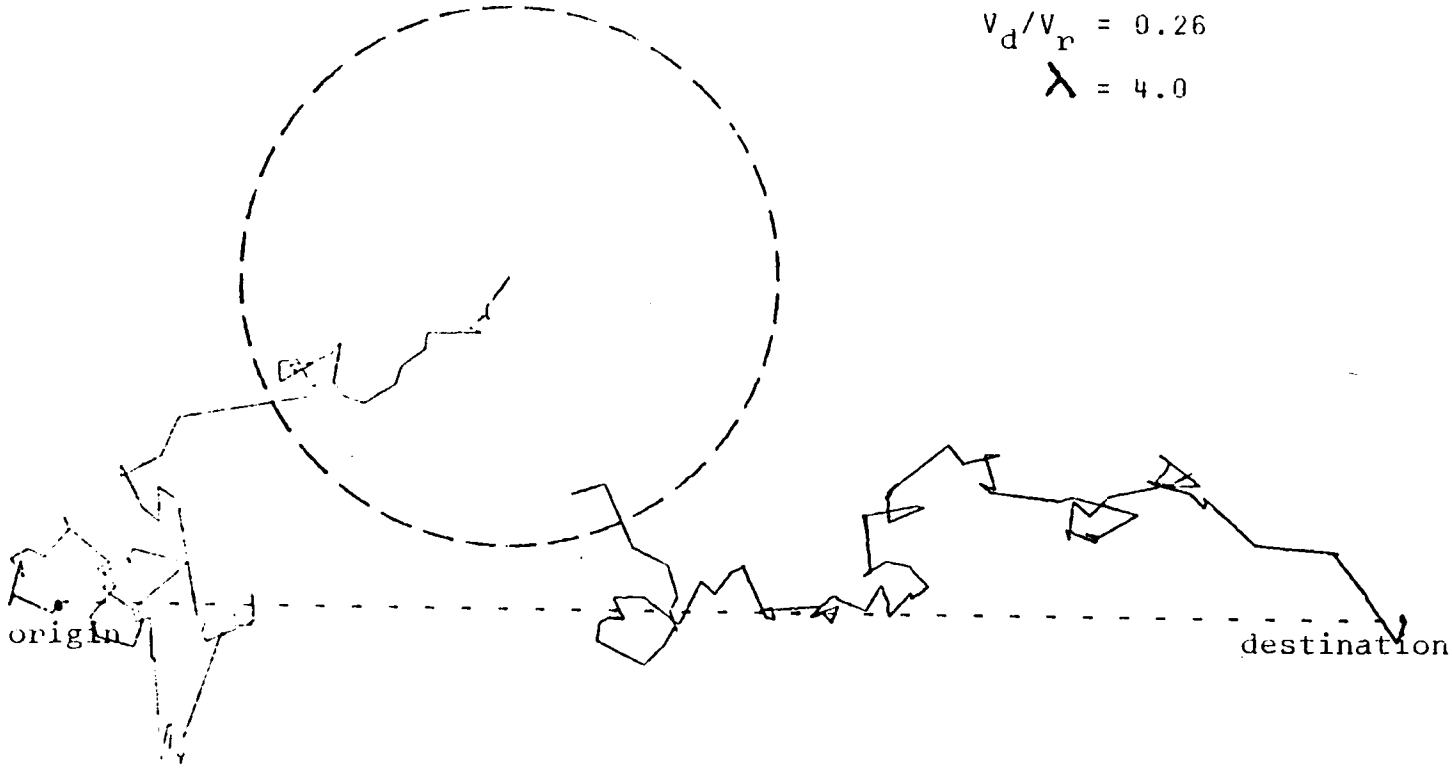

fixes. Of course, any method for devising a path under such constraints is bound to fail. A target cannot randomize its motion if it must travel directly to its destination. The rejection of the path in Figure 4a is not a rejection of the idea of random tour with drift, but only of the constraints. Even though 2.69 is in the low end of the range of V_d/V_r, any ratio greater than about 1.50 produces paths that are unacceptable. In Figure 4b, where the ratio is 1.13, the path is still highly constrained but looks much better. The drift constraint really begins to loosen in Figure 4c, and in Figures 4d-f the ratio is 0.26. Here, the randomizing qualities of the random tour are evident. The paths all "look good", and whether they are executable by a target depends only upon what the time and distance units are. For instance, if the time unit is one half hour, Figure 4f has the target turning every 7.5 minutes on the average. This turn rate is not realistic for a large target. However, the path in Figure 4d has a mean turn rate of two per hour and is certainly executable. The main concern at this point has been put to rest; the paths in Figures 4c-f for which the time constraints are reasonable, look good enough to warrant further evaluation.

The next measure of effectiveness against which to evaluate the random tour with drift is the distribution of the magnitude of difference between present course and course from present position to destination, measured at specified

times during path generation. This measure is discussed in Chapter II and is illustrated in Figure 1a. Recall now the procedure for generating each leg of the tour. The direction of the randomizing velocity ($\vec{V}_r$) is selected by making a draw from a uniform (0,2π) distribution, and its magnitude is determined by multiplying the randomizing speed (determined from desired target speed through the water and drift, as in Figure 2) by the time length of the leg selected from an exponential (λ) distribution. While the distribution of the direction of the randomizing velocity may be uniform, the distribution of the direction of the velocity through the water is not. The solid spokes of the left circle in Figure 10a represent randomizing velocity and are equally spaced angularly. The dashed spokes of the right circle in Figure 5a represent the water velocity after the appropriate drift velocity is added, and are not equally spaced angularly. The angle (θ_1) that any water velocity vector ($\vec{V}_w$) forms with the x axis is a function of the angle (θ_θ) of the randomizing velocity, the drift speed, and the randomizing speed. In Figure 5b;

$$r = V_r / \lambda \qquad d = V_d / \lambda,$$

where the randomizing velocity required to cause the desired mean water velocity, as derived in (9) and (10), is,

$$V_r = (V_w^2 - V_d^2)^{1/2}$$

because the mean angle between randomizing velocity and course from present position to destination is 90 degrees. The x and y components of the randomizing velocity are;

$$x_0 = r\cos\theta_0 \qquad y_0 = r\sin\theta_0$$

and the x and y components of the water velocity are;

$$x_1 = x_0 + d \qquad y_1 = y_0.$$

Now,

$$\tan\theta_1 = y_1/x_1$$

$$\tan\theta_1 = y_0 / (x_0 + d)$$

$$= (((V_r/\lambda)\sin\theta_0) / [((V_r/\lambda)\cos\theta_0) + d])$$

$$= \sin\theta_0 / [\cos\theta_0 + (V_d/V_r)].$$

And finally,

$$\theta_1 = \arctan(\sin\theta_0 / [\cos\theta_0 + (V_d / V_r)]) \qquad (17)$$

Notice that the redistribution of courses is not a function of lambda, but is strictly dependent on the ratio V_d/V_r.

Even having the distribution of θ_0 and knowing θ_1 as a function of θ_0, obtaining the density of θ_1 by mathematical analysis is very difficult, but can be circumvented somewhat satisfactorily by using Monte Carlo simulation. It is a simple matter to draw several hundred random numbers from a uniform (0,2π) distribution and then tranform them with (17). This procedure was executed and the results appear in Table 1

Figure 5:

Effect of Drift on Course Distribution

Figure 5a:

Redistribution of Courses After the Addition of Drift

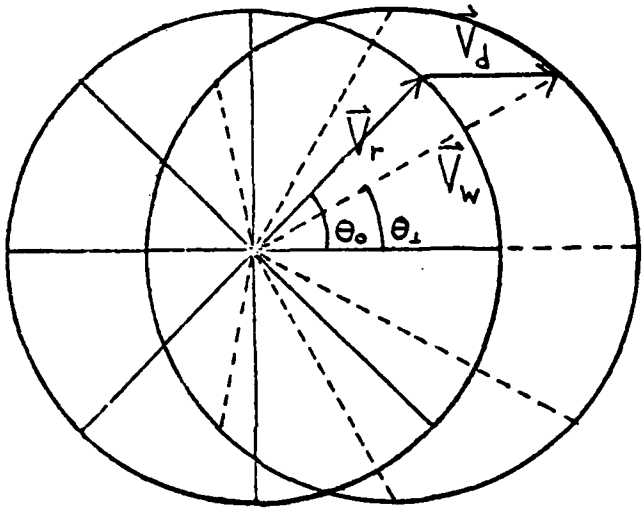

Figure 5b:

Representation of Course Angular Shift

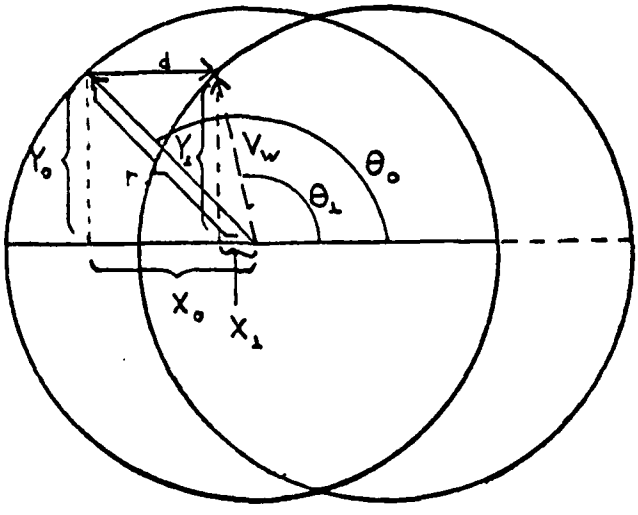

compared with the statistics obtained during path generation. Some significant observations are:

1. The mean magnitude of the difference between present course and course to destination obtained from path statistics, and the associated standard deviation, agree very closely with the statistics obtained for θ_1 by the simple simulation described above. This result was anticipated because the expected position of all experimental paths lies on the baseline even though very few actual positions fall there. However, and very importantly, Figures 6a, b, c and 7a indicate that there is a strict maximum deviation angle for any V_d/V_r ratio. This is true only if the drift vector points directly from present position to destination all the time. If position is always on the baseline (where the mean position for the entire process lies) then a maximum deviation will exist and will be arcsin (V_r/V_d), a fact which Figure 7a makes convincing. However, during travel the target deviates above and below the baseline, and though there is a maximum angle between the drift vector and water vector, to this angle must be added the depression or elevation angle between the horizontal and the destination. For example, if the target's x-axis distance from destination is 10 units, as is also the y-axis

Table 1:

Random Tour Statistics for Deviation Between Present Course and Course from Present Position to Destination

		random tour deviations in degrees						path generated		simulated from (17)	
		mean			standard deviation			avg.mean for all lambda	avg.std.dev. all lambda	avg.mean for all lambda	avg.std.dev. all lambda
V_d/V_r	lambda	left	cleft	right	left	cleft	right	this V_d/V_r	this V_d/V_r	this V_d/V_r	this V_d/V_r
2.69	1.0	14.31	14.11	14.04	7.10	6.99	6.86				
"	2.0	13.78	13.92	13.23	7.01	6.89	6.95	13.82	6.94	13.04	6.79
"	4.0	13.54	13.73	13.76	6.96	6.93	6.85				
1.13	1.0	39.6	39.6	38.7	21.0	19.5	20.0				
"	2.0	39.5	41.4	35.8	21.4	21.7	21.0	38.49	20.48	35.15	19.37
"	4.0	38.19	38.27	35.75	19.43	18.93	19.68				
0.55	1.0	73.3	73.1	70.7	47.7	47.7	48.0				
"	2.0	73.5	69.9	71.1	47.4	45.0	48.0	69.99	47.38	66.17	47.34
"	4.0	68.6	68.32	66.75	46.77	46.54	46.72				
0.253	1.0	84.9	79.23	83.32	51.24	49.14	51.0				
"	2.0	82.33	79.71	75.66	53.13	50.02	49.76	80.81	50.44	78.18	51.14
"	4.0	81.57	80.61	78.94	50.93	51.43	50.09				

-distance, and the target is above the baseline, then the angle between the horizontal line going through the target and the line going between target and destination is 45 degrees. Now, the next leg out of that position might form the maximum angle [arcsin (V_r/V_d)] between it and the drift direction. Then, the pointing deviation which we are interested in is the sum of those two angles = 45 degrees + arcsin (V_r/V_d). Nonetheless, the mean pointing deviation angles and their standard deviations are remarkably similar for the simulated paths and the simulation of $f(\theta_1)$, where one set of statistics is for the true distribution of courses and the other is for the conditional distribution given present position equal to mean target position.

2. No significant difference is noted between the mean differences for left unclipped, left clipped, and right paths. This is evidence that not only are left and right matching paths symmetrical in distribution, but more notably that clipping the left side by constraining it to match a right side path has no effect on the frequency with which the target points at its destination.

3. Lambda, as expected, has no effect on course distribution; only the ratio V_d/V_r does.

Figures 6a-c show the distributions of simulated course deviations for high, medium and low ratios. Notice that for a high ratio, greater than one in this context and signifying tight constraints, the distribution loads on the higher values, while for ratios less than one, signifying loose contraints, on the lower values. The break point occurs when the ratio is equal to one. While this loading, first on one end of the distribution range and then on the other, seems odd at first blush, there is a reasonable explanation for it that Figure 7 helps to illustrate. For high ratios the tranformation of θ_0 to θ_1 causes a high proportion of the arc length of the circle described by the maximum V_r to be subtended by the higher values of θ_1. Figure 7a illustrates this occurence and also provides a graphical representation of why maximum values of course deviation are low for high ratios. As the ratio gets larger, the drift vector in the positive x direction accounts for an increasing amount of the water velocity, causing the circle described by the maximum magnitude of the randomizing velocity to grow smaller. Notice also that when $V_d = V_r$ (Figure 7b) the maximum course deviation is 90 degrees and all feasible values are equally distributed because they subtend equal amounts of arc length. When the ratio is any greater than one, it is immediately feasible to have deviations as great as 180 degrees, the maximum possible. However, the higher deviation values subtend less arc length of the circle described by maximum V_r

Figure 6a:
Simulated Distribution of Course Deviations

$V_d/V_r = 2.69$

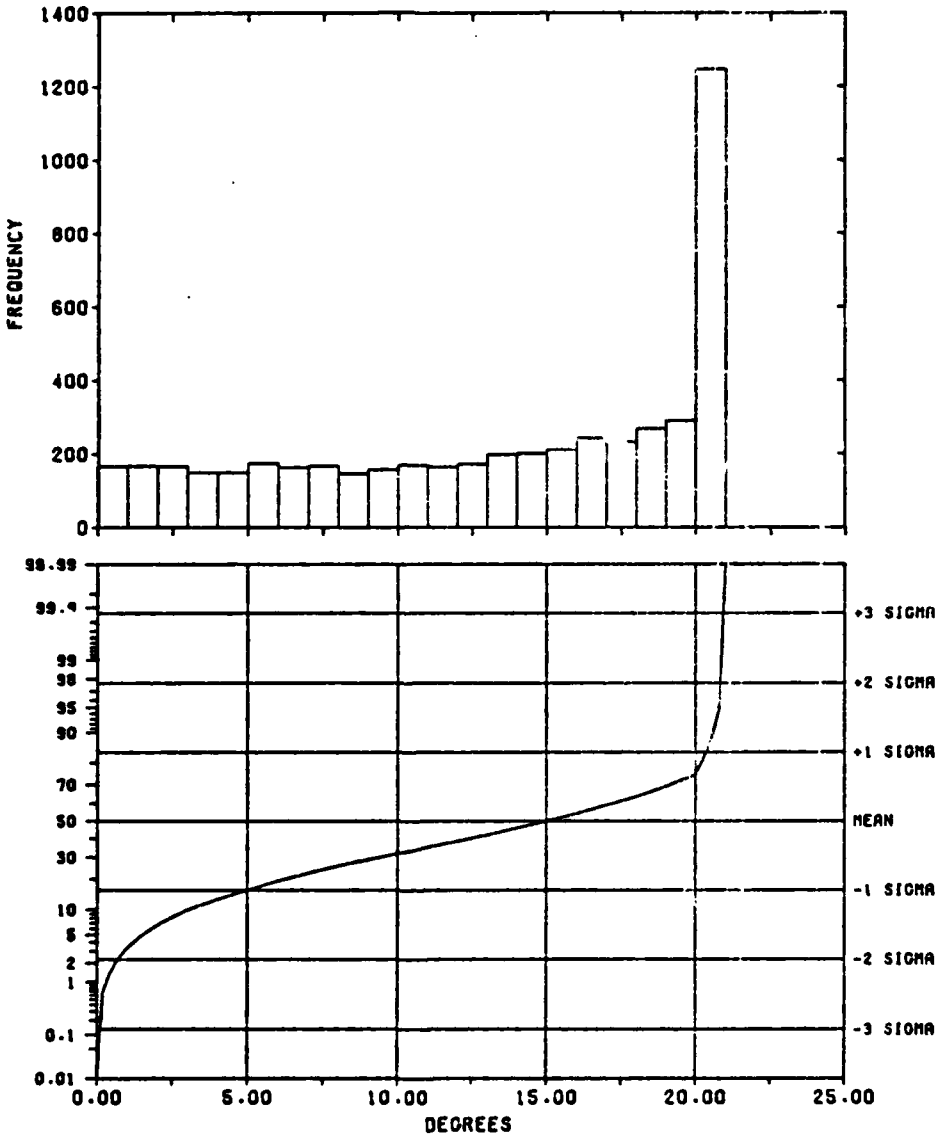

MEAN = 1.304E1 MIN = 0.000E0 CELL = 1.000E0
SIGMA = 6.786E0 MAX = 2.100E1 #CELLS = 21
#POINTS = 5000

Figure 6c:

Simulated Distribution of Course Deviations

V_d/V_r = 0.26

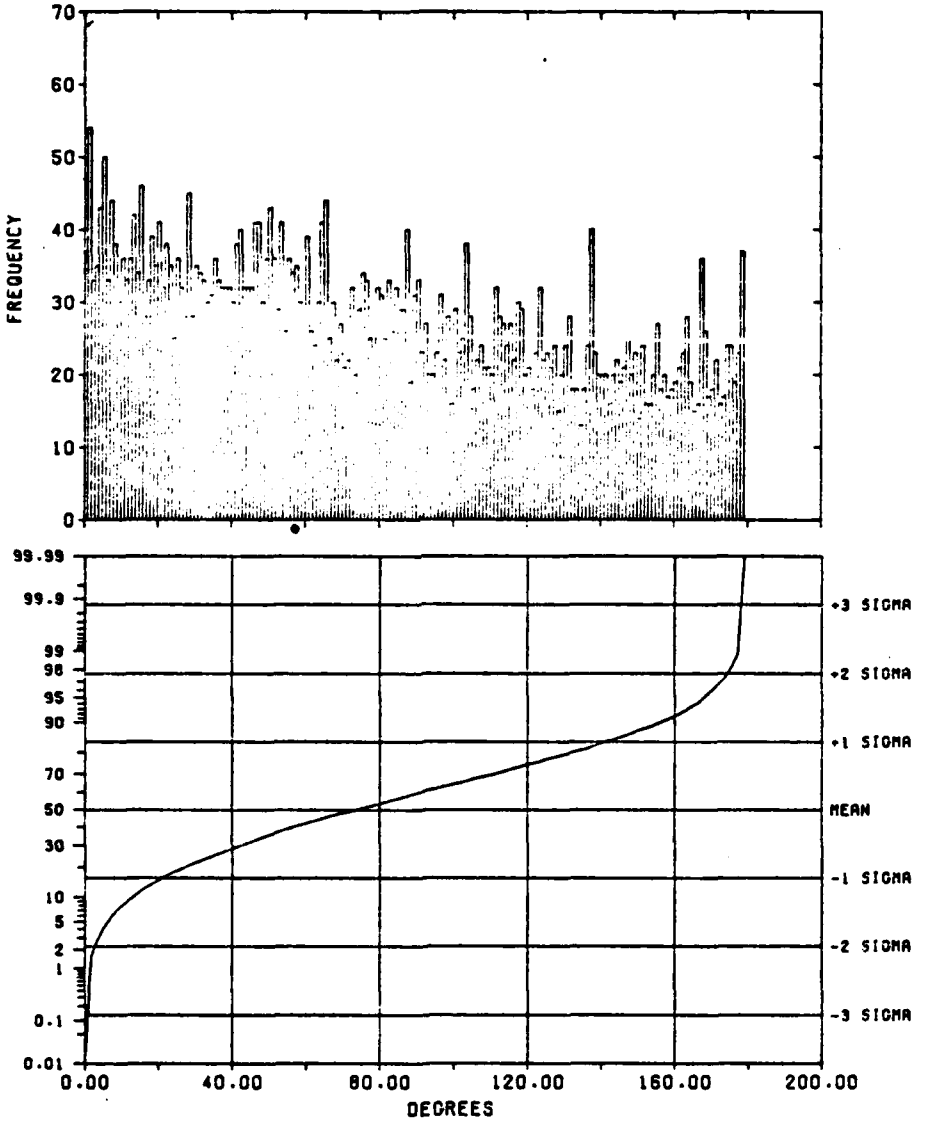

MEAN = 7.838E1 MIN = 0.000E0 CELL = 1.000E0

SIGMA = 5.144E1 MAX = 1.790E2 #CELLS = 179

#POINTS = 5000

Figure 6b:

Simulated Distribution of Course Deviations

$V_d/V_r = 1.0$

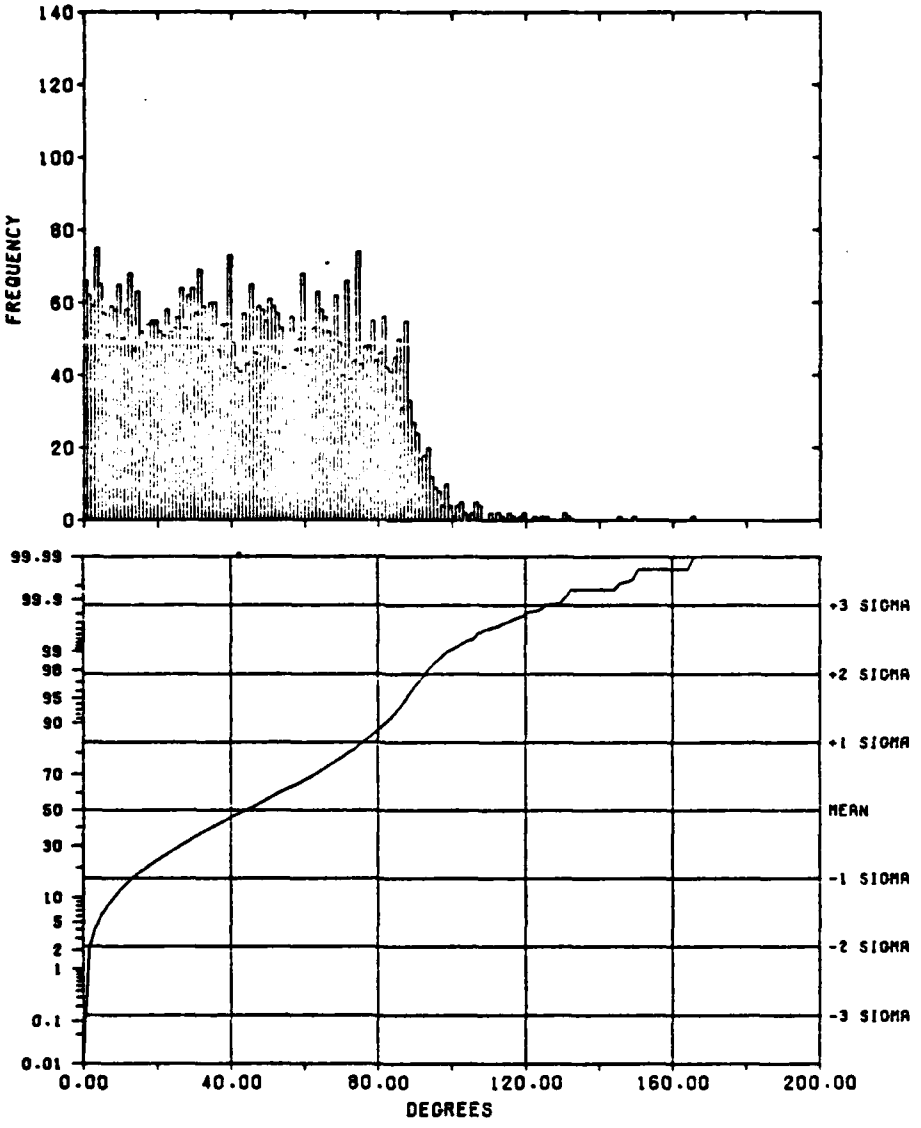

MEAN = 4.428E1 MIN = 0.000E0 CELL = 1.000E0

SIGMA = 2.725E1 MAX = 1.660E2 #CELLS = 166

#POINTS = 5000

Figure 7:

Redistribution of Courses After the Addition of Drift

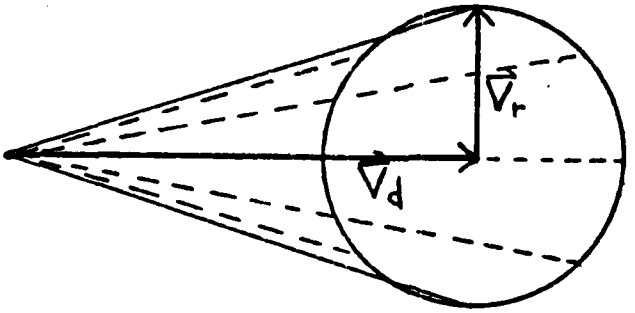

Figure 7a:
$V_d > V_r$

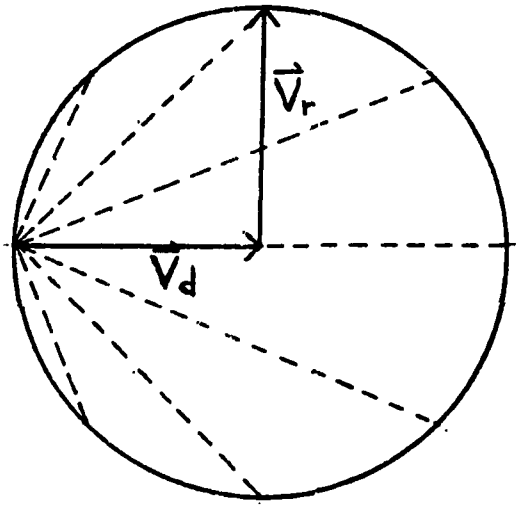

Figure 7b:
$V_d = V_r$

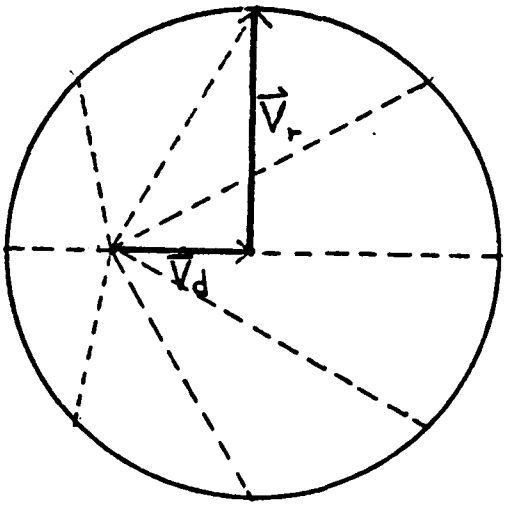

Figure 7c:
$V_d < V_r$

than do the smaller values, as illustrated in Figure 7c. Recall though that these distributions are not actual course deviation distributions determined from generating actual paths, but are conditional course distributions given that present positon equals baseline position (which is expected position of target over all possible paths). However, and most importantly, the mean and standard deviation of the actual path course deviation distribution can be determined using this simple inexpensive simulation once V_d and V_r are specified. Thus, the target knows how much it tends to point at its destination or away from its origin.

As detailed in Chapter II, the third measure of effectiveness is mean square radial distance between present position and baseline position. If the density of the course distribution after the application of drift [$f(\theta_t)$] had been obtained, then $E[R_t^2]$ could be easily calculated for any time making the appropriate substitutions into (4) and (5). Again, however, the derivation of the density of θ_1 is very difficult and not necessary because the process can be viewed as a random tour carried out at the randomizing velocity, merely shifted right or left by drift velocity prorated for cumulative run time. At any time, the "origin" of this process, viewed as a driftless random tour with velocity V_r, is the baseline position. This way, $E[R_t^2]$ is calculated by substituting V_r and t directly into (4). However, the resulting figures can only be compared validly to the

experimental statistics obtained for the unclipped left side; the requirement for left and right sides to match adds a further constraint that is not captured by a process that is merely an unconstrained random tour appropriately shifted for drift. Thus, the statistics for the matching paths must first be compared to each other in order to test for symmetry and then compared to the experimental statistics for the unclipped left side, which themselves have been compared to the figures obtained from (4). All these comparisons were made with the following significant results:

1. Experimental statistics for both the left and right matching paths support the assertion that both sides are symmetrical.
2. Experimental statistics for the unclipped left path mean square radial distance agree very closely with the analytical figures obtained by substituting V_r into (4). Experimental figures tend to be one to three percent higher, but any difference that small is acceptable as sampling error. Mean square radial distance grows with time, and for a given time t is less for greater lambda, as expected. Table 2 summarizes the statistics for the various time checks. 'Cleft' denotes clipped left paths, 'left' denotes unclipped left paths, 'actual' means obtained from path simulation, and 'expect' means obtained from equation

(4) by substitution of appropriate V_r. The holes in the table occur because, at lambda equal to one or two, checks were not made for all times listed. Nonetheless, more than enough statistics were obtained to provide valid results.

3. The ratios of experimental clipped/experimental unclipped mean square radial distance were calculated for the left paths and are summarized in Table 3. Linear least squares regression of the ratios against time indicates that mean square radial distance reduction caused by clipping (requiring a match with the right side path) is independent of V_d and lambda but dependent on time. The mean reduction is about two per cent per time unit with a standard deviation of approximately 1.2 per cent over the range for which the regression was done. On this range a linear fit is quite good, but notice that after fifty time units the linear reduction results in a mean square radial distance of zero, which is ridiculous because it is out of range for the regression. Clearly, the reduction caused by requiring the right and left paths to match must be calculated over the appropriate range. Though two per cent does not sound like much of a loss, it becomes quite significant after awhile, as will be demonstrated when the random tour with drift compared with Brownian motion. Nonetheless, it is clear that

Table 2:

Mean Square Radial Distance from Baseline Position at Time t for Random Tour with Drift

			time													
			1.73			3.45			5.18			6.91			8.6		
V_d/V_r	lambda	path	actual	expect	a/e	actual	expect	a/e	actual	expect	a/e	actual	expect	a/e	actual	expect	a/e
4.10	1.0	left										23.20	22.91	0.97			
3.63	"	cleft										20.34	22.91	0.89			
3.77	2.0	left				5.28	5.72	0.92				12.94	12.42	1.04			
3.39	"	cleft				5.50	5.72	0.96				11.15	12.42	0.90			
3.63	4.0	left	1.21	1.43	0.84	3.09	3.10	1.00	4.02	4.78	0.97	6.55	6.45	1.01	8.74	8.12	1.07
3.28	"	cleft	1.14	1.43	0.80	2.96	3.10	0.95	4.28	4.78	0.90	6.26	6.45	0.97	8.11	8.12	1.00
1.55	1.0	left										85.18	82.75	1.03			
1.47	"	cleft										80.85	82.75	0.98			
1.57	2.0	left				21.31	20.55	1.06				49.22	44.87	1.10			
1.51	"	cleft				19.87	20.55	0.96				33.35	44.87	0.74			
1.55	4.0	left	5.39	5.16	1.04	11.60	11.20	1.04	18.65	17.26	1.08	25.36	23.31	1.09	32.58	29.33	1.11
1.43	"	cleft	5.12	5.18	0.99	9.48	11.20	0.85	13.87	17.26	0.80	17.82	23.31	0.76	20.10	29.33	0.69
0.63	1.0	left										146.11	146.86	1.03			
0.63	"	cleft										139.00	141.86	0.98			
0.63	2.0	left				37.20	35.41	1.05				68.34	76.92	1.12			
0.61	"	cleft				37.31	35.41	1.05				76.09	76.92	0.99			
0.63	4.0	left	9.88	8.83	1.11	21.42	19.20	1.12	29.04	29.59	1.01	43.75	39.96	1.02	52.10	50.20	1.04
0.63	"	cleft	8.93	8.83	0.94	17.30	19.20	0.90	24.53	29.58	0.83	31.56	39.96	0.79	38.99	50.29	0.78
0.26	1.0	left										175.71	177.34	1.05			
0.26	"	cleft										176.08	177.33	0.99			
0.26	2.0	left				48.33	44.26	1.09				105.42	96.15	1.11			
0.25	"	cleft				43.46	44.25	0.91				90.71	96.15	0.94			
0.26	4.0	left	11.34	11.10	1.02	24.99	24.00	1.04	39.67	36.98	1.07	54.76	49.95	1.09	65.37	62.15	1.04
0.26	"	cleft	11.82	11.10	1.06	23.77	24.00	0.99	39.12	36.99	1.05	51.08	49.95	1.02	59.45	62.35	0.95

Table 2 (continued):

Mean Square Radial Distance from Baseline Position
at Time t for Random Tour with Drift

			time															
			10.35			12.09			13.82			15.54			17.27			
V_d/V_r	lambda	path	actual	expect	a/e	actual	expect	a/e	actual	expect	a/e	actual	expect	a/e	actual	expect	a/e	
4.14	1.0	left							51.16	49.68	1.03							
3.63	"	cleft							43.16	49.68	0.87							
3.77	2.0	left	19.78	19.08	1.04				25.61	25.81	0.99				33.06	32.49	1.02	
3.39	"	cleft	16.62	19.08	0.87				21.06	25.81	0.82				24.56	32.49	0.76	
3.53	4.0	left	9.90	9.78	1.01	11.96	11.47	1.04	14.04	13.15	1.07	17.22	14.81	1.16	19.26	16.49	1.17	
3.26	"	cleft	8.87	9.78	0.91	10.12	11.47	0.88	11.58	13.15	0.85	15.18	14.81	1.02	16.86	16.49	1.02	
1.55	1.0	left							195.52	179.48	1.09							
1.47	"	cleft							129.96	179.48	0.72							
1.57	2.0	left	89.04	68.95	1.29													
1.61	"	cleft	58.69	68.95	0.85													
1.54	4.0	left																
1.49	"	cleft																
.63	1.0	left							338.09	307.68	1.10							
.63	"	cleft							291.71	307.68	0.95							
.63	2.0	left	125.34	118.20	1.06				174.51	159.84	1.09							
.61	"	cleft	87.64	118.20	0.74				138.28	159.84	0.68							
.63	4.0	left	55.15	60.60	0.99	73.83	71.04	1.04										
.63	"	cleft	40.41	60.60	0.67	46.58	71.04	0.65										
.25	1.0	left							427.[illegible]	384.60	1.11							
.25	"	cleft							352.04	384.60	0.92							
.25	2.0	left	147.82	147.75	1.00				[illegible]21.16	199.80	1.01				252.95	251.[illegible]	1.[illegible]	
.26	"	cleft	112.56	147.75	0.76				146.48	199.80	0.74				188.43	251.[illegible]	[illegible]	
.26	4.0	left	76.46	75.75	1.01	95.07	88.80	1.07	105.10	101.78	1.03	120.03	114.68	1.05	134.45	127.65	1.05	
.26	"	cleft	69.56	75.75	0.92	83.79	88.80	0.94	87.67	101.78	0.86	96.72	114.68	0.84	101.32	127.65	0.79	

Table 2 (continued):

Mean Square Radial Distance from Baseline Position
at Time t for Random Tour with Drift

			time																	
			19.00			20.73			22.45			24.18			25.90					
V_d/V_r	lambda	path	actual	expect	a/e	actual	expect	a/e	actual	expect	a/e	actual	expect	a/e	actual	expect	a/e			
4.10	1.0	left				77.96	76.45	1.02												
3.63	"	cleft				58.24	76.45	0.76												
3.77	2.0	left				40.43	39.20	1.03												
3.39	"	cleft				28.49	39.20	0.73												
3.63	4.0	left	22.04	18.16	1.21	23.56	19.84	1.19	24.43	21.51	1.14									
3.28	"	cleft	19.48	18.16	1.07	20.04	19.84	1.05	21.05	21.51	1.00									
1.55	1.0	left				324.50	276.22	1.17												
1.47	"	cleft				164.20	276.22	0.59												
1.57	2.0	left																		
1.61	"	cleft																		
1.51	4.0	left																		
1.48	"	cleft																		
.63	1.0	left				494.62	473.52	1.04												
.65	"	cleft				346.68	473.52	0.73												
.63	2.0	left																		
.61	"	cleft																		
.63	4.0	left																		
.63	"	cleft																		
.26	1.0	left				626.41	591.90	1.06												
.26	"	cleft				393.70	591.90	0.67												
.25	2.0	left				309.87	303.45	1.02				378.24	355.20	1.06						
.26	"	cleft				222.40	303.45	0.73				243.31	355.20	0.68						
.26	4.0	left	147.29	140.63	1.05	158.95	151.60	1.03	178.87	166.50	1.07	194.50	179.46	1.08	207.38	192.3[illegible]	1.08			
.26	"	cleft	112.52	140.63	0.80	116.00	151.60	0.76	118.49	166.50	0.71	125.77	179.45	0.70	134.02	192.33	0.70			

Table 3: Ratio of Left Clipped/Left Unclipped Mean Square Radial Distance at Time t for Random Tour with Drift

V_d/V_r	lambda	3.45	6.91	10.35	hour 13.82	17.27	20.73	24.18
2.69	1.0		.92		.84		.75	
"	2.0	1.04	.86	.84	.82	.74	.70	
"	4.0	.96	.94	.90	.85	.88	.88	
1.13	1.0		.95		.66		.51	
"	2.0	.91	.68	.66				
"	4.0	.82	.70					
0.58	1.0		.95		.86		.70	
"	2.0	1.00	.89	.70	.62			
"	4.0	.81	.77	.67				
.258	1.0		.95		.82		.63	
"	2.0	.84	.76	.76	.74	.70	.72	.64
"	4.0	.95	.95	.91	.83	.75	.73	.65

mean square radial distance for any path, given drift speed, randomizing speed, and lambda, is very predictable.

B. BROWNIAN-DERIVED MOTION

Again, the first measure of effectiveness addresses how representative paths produced by a method "look", and Figures 8a-g are representative of discrete Brownian-derived motion as executed by the second procedure delineated in Chapter IV. The paths in Figures 8a-d "look" acceptable; they show no pattern of regularity and seem to be executable, depending on the time and distance units selected. Figures 8a and 8b were generated from identical random numbers, V_d/V_r ratio, $\lambda = 1.0$, and maximum and minimum water speeds. The only difference between them is the physical parameter σ^2 which is 5.0 for Figure 8a and 10.0 for Figure 8b. The paths look quite similar but do not look different enough for one to speculate about possible differences for the other two measures of effectiveness. It is worth noting that for $\sigma^2 = 5.0$ there are more extentions and less clips than than for $\sigma^2 = 10.0$. This result is to be expected because a higher variance in the normal draws in (16) should produce successive positions that are farther apart than those produced with a lesser variance. When mean square radial distance is discussed later, the amount of clipping and extending which takes place becomes significant, generally

Figure 8a: PLOT OF DISCRETE BROWNIAN-DERIVED MOTION

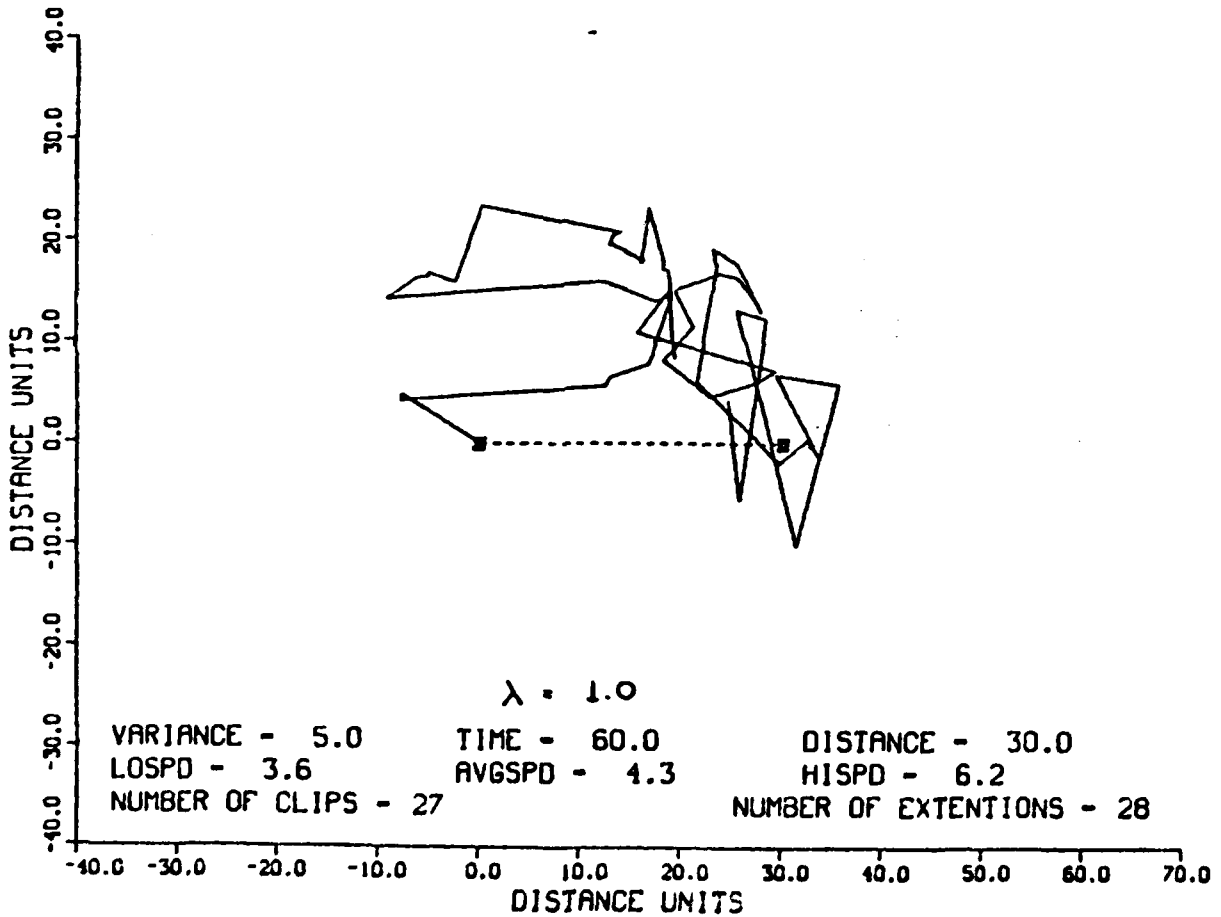

Figure 8b: PLOT OF DISCRETE BROWNIAN-DERIVED MOTION

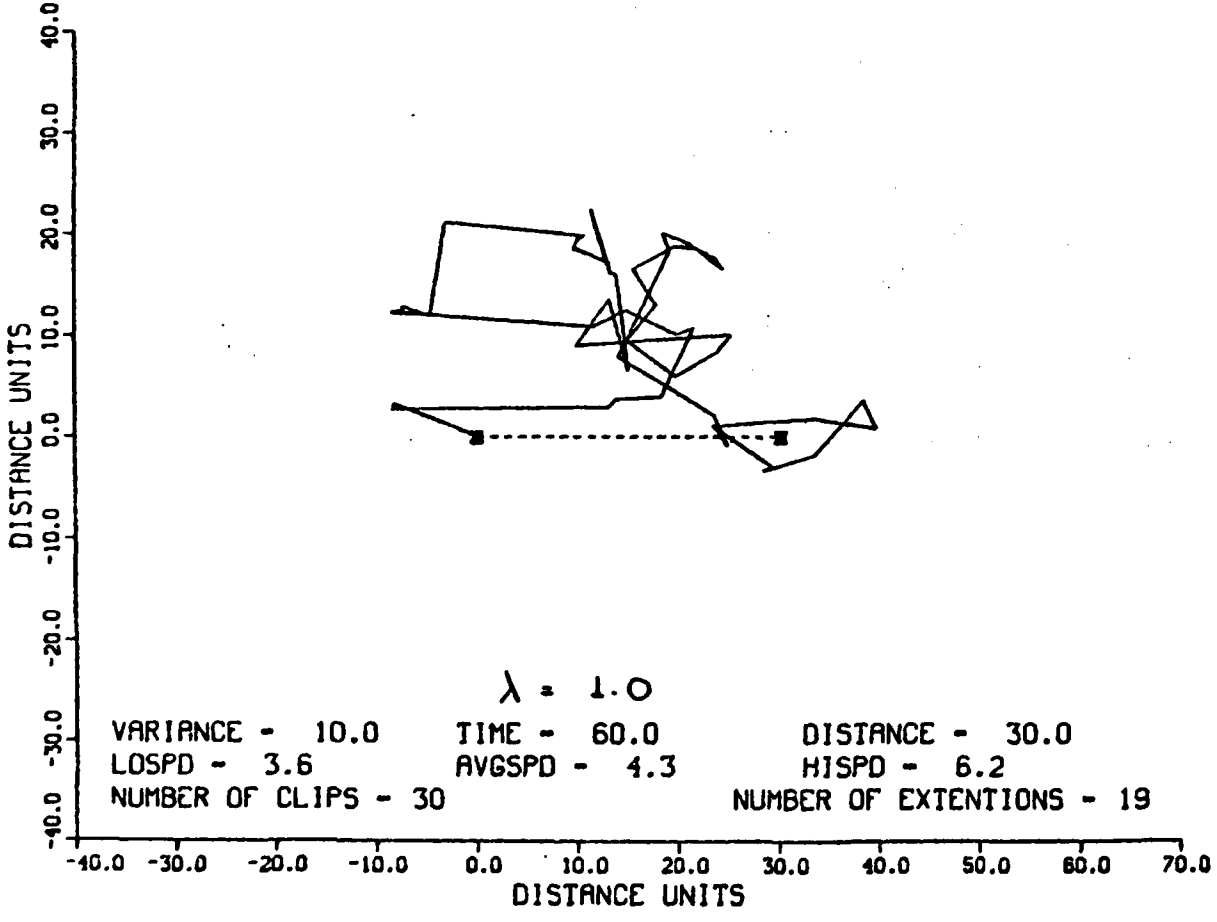

Figure 8c: PLOT OF DISCRETE BROWNIAN-DERIVED MOTION

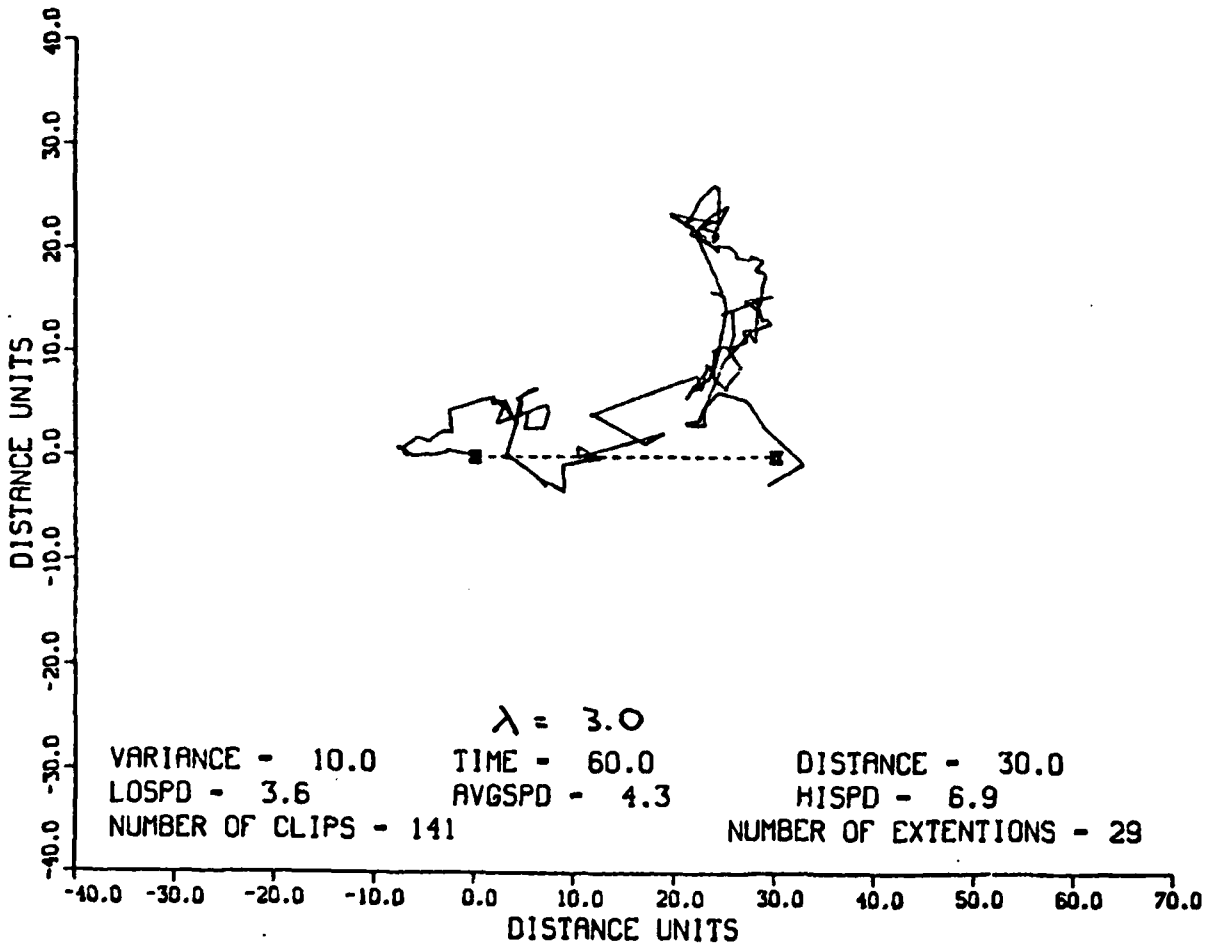

Figure 8d: PLOT OF DISCRETE BROWNIAN-DERIVED MOTION

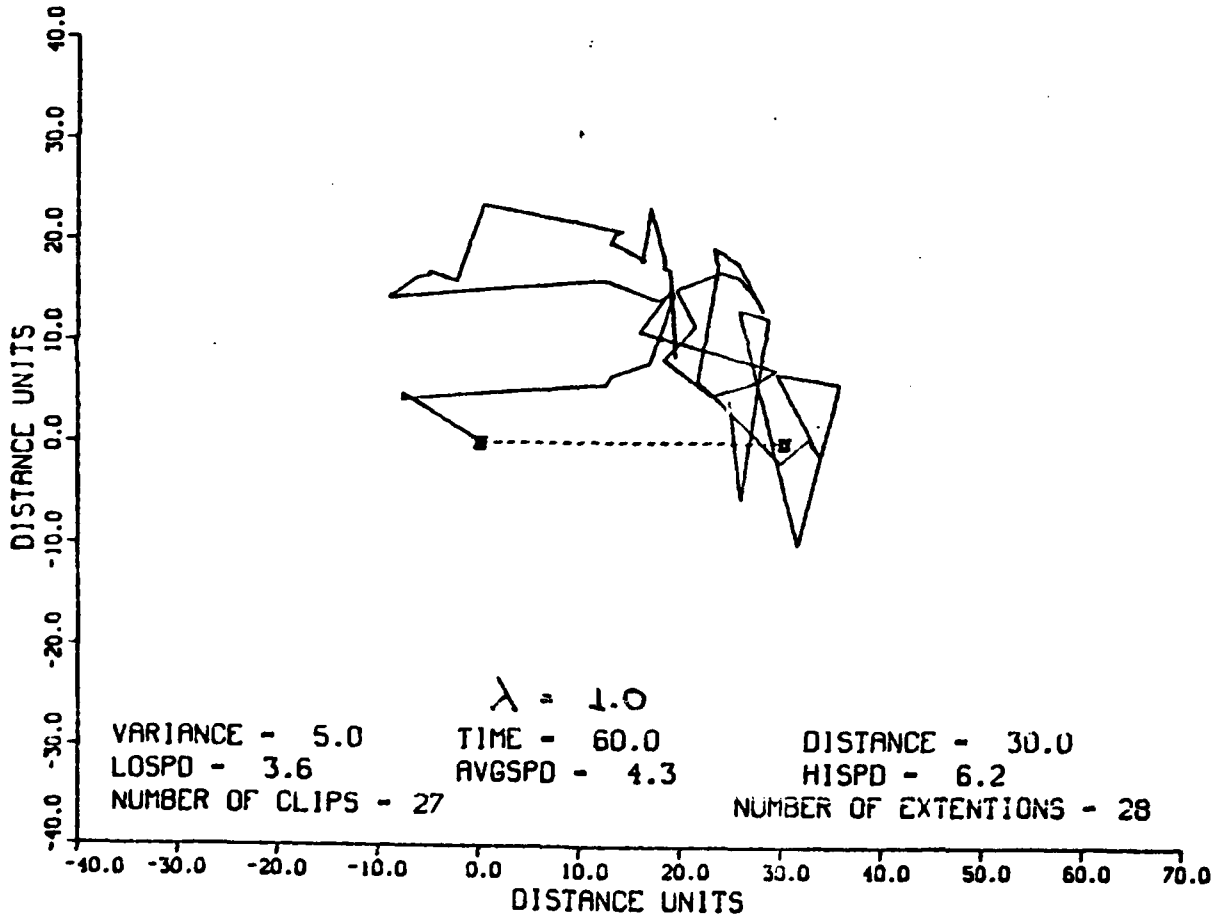

Figure 8e: PLOT OF DISCRETE BROWNIAN-DERIVED MOTION

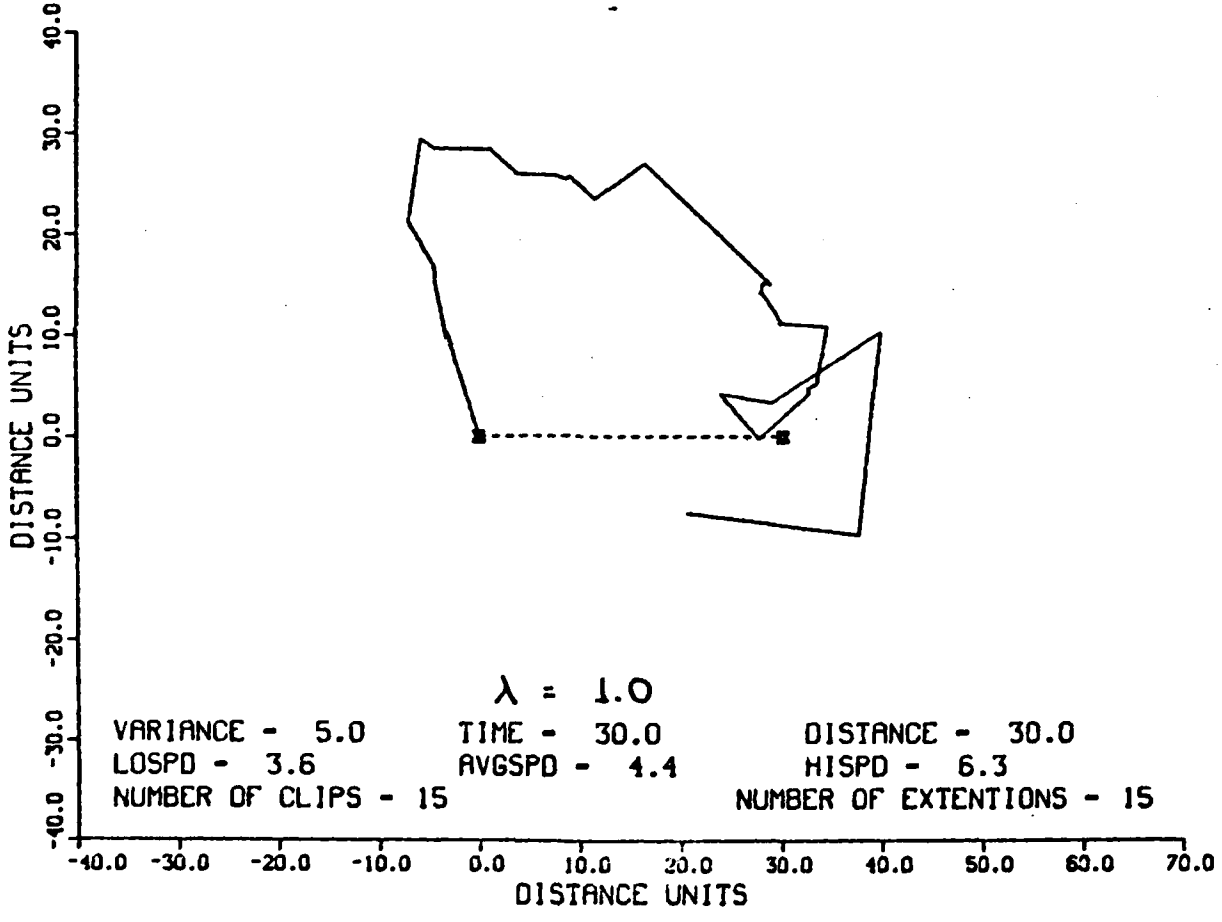

Figure 8f: PLOT OF DISCRETE BROWNIAN-DERIVED MOTION

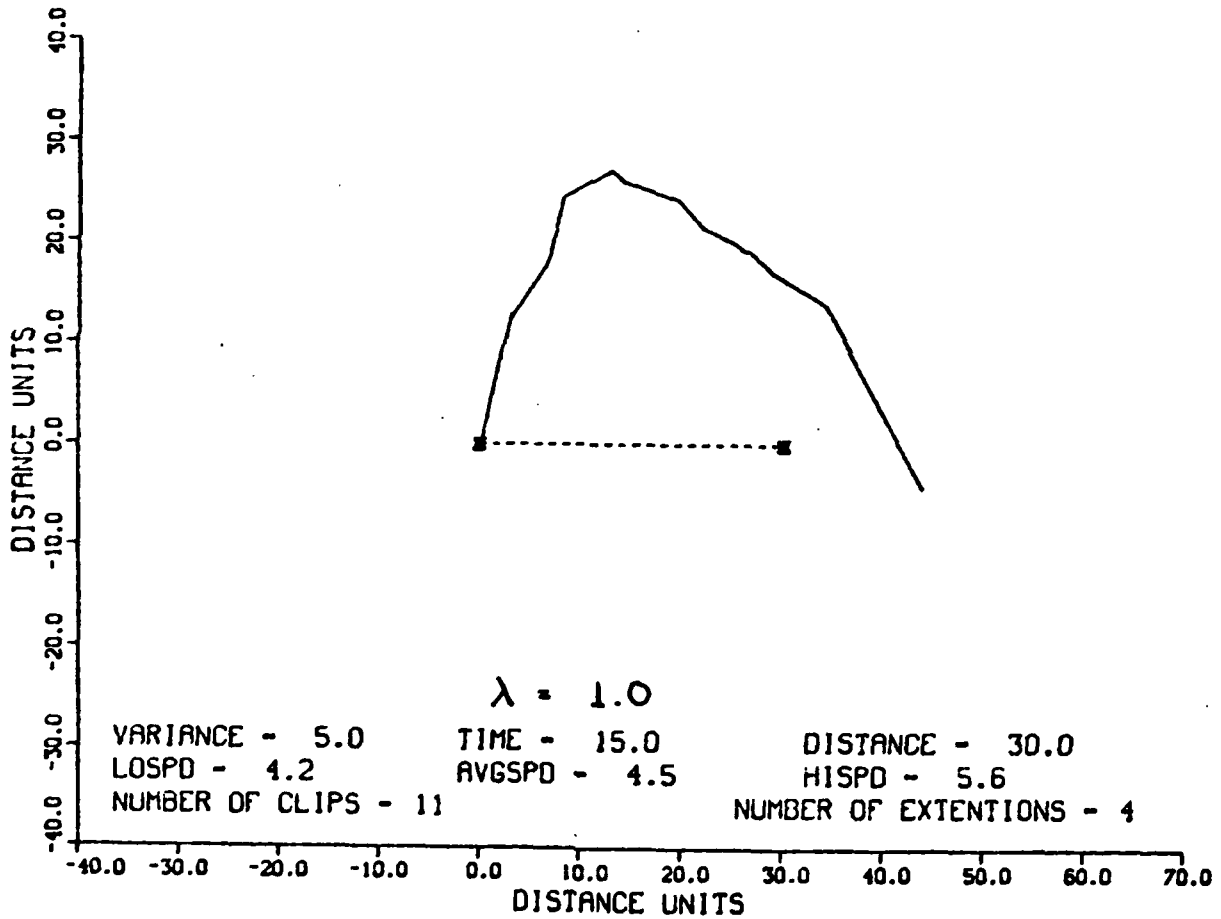

Figure 8g: PLOT OF DISCRETE BROWNIAN-DERIVED MOTION

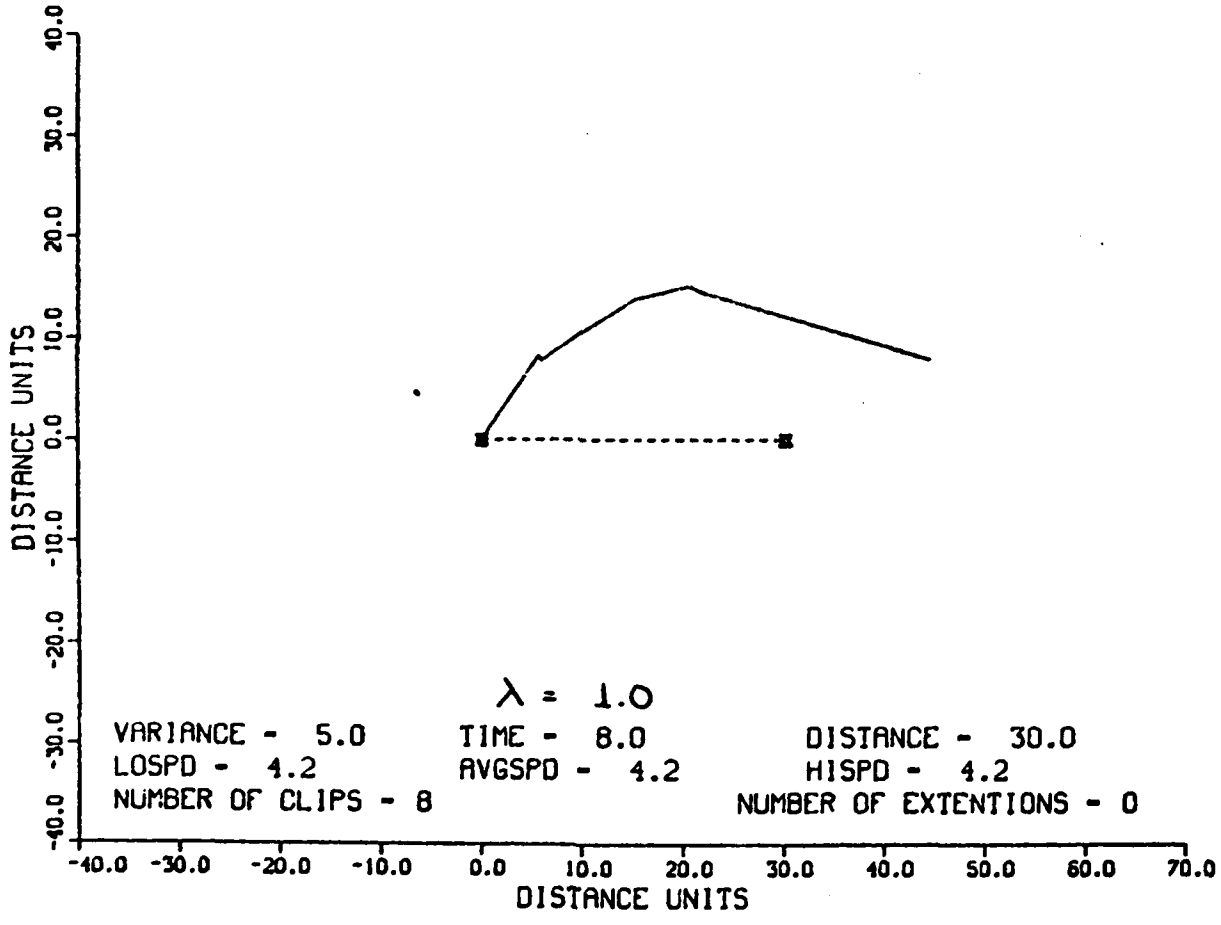

causing the difference for that statistic for two different σ^2 to be reduced.

Figures 8b and 8c were produced with similar inputs except for lambda, which is 1.0 and 3.0 respectively. The difference between these paths is readily apparent, but again it is impossible from one example for each set of inputs to draw any general conclusions about the effect of turning rate on other two measures of effectiveness. Figures 8d-g were generated from identical inputs with the exception of V_d/V_r which is 0.12, 0.23, 0.5, and 1.98 respectively. As the ratio becomes higher the paths straighten out as expected. The path in Figure 8g does not "look" acceptable, which is no surprise given the strict contraints. Random tour paths with similarly high ratios suffered the same straightening. Notice also, that as the ratio becomes high the process is more constrained but less likely to obey the constraints. The goal of the original controlled time of arrival problem was to assure that the target started from an origin and visited the destination at the end of the stated time period. It is clear in all four of Figures 8d-g that the constraints are violated, and furthermore, that as the V_d/V_r ratio increases the constraints are violated more. For any path that does not end at the destination there remains three options. First, it can be rejected outright. Secondly, it is possible that the requirement to reach the destination exactly is not as important as ending the path on time, in

which case, the path is acceptable if it is not too straight. Lastly, if the time constraint is not as important as ensuring that the target visits the exact destination, then more time can be given to the target with which to travel directly to destination if the distance is not great. The problem of control will be the subject of further comment when mean square radial distance from baseline position is examined. It suffices at this point to recognize that the problem exists and will probably affect the other two measures of effectiveness.

The second measure of effectiveness quantifies how much a target points directly away from its origin and to its destination. For the random tour it was found that the amount of pointing, as measured by the magnitude of the angle between the target's present course and the course to the destination from present position, was a function only of the ratio V_d/V_r, and not a function of time or turning rate lambda. Those results provide a starting point for the investigation of pointing for Brownian-derived motion. Histograms of the deviation angle appear for high, medium, and low V_d/V_r ratios for Brownian-derived motion in Figures 9a-c, and Table 4 lists the statistics for three σ_2 values and six ratios. The table also lists values of pointing statistics for the random tour with drift obtained during path generation. Significant results are:

1. The amount of pointing for Brownian-derived motion agrees very closely with that for the random tour with drift for low V_d/V_r ratios, as exhibited in Table 4. This result is expected because, regardless of the method chosen for generating paths, a drift velocity will bias course headings in the direction of the destination. Brownian-derived motion with the same V_d/V_r ratio as a random tour should exhibit similar pointing behaviour.

2. Table 4 also shows that as the drift/randomizing ratio increases the pointing statistics for the two different processes begin to diverge. While the random tour statistics continue to agree closely with those generated by the simulation of (17), the Brownian-derived motion statistics decrease to a mean of approximately 56 degrees and standard deviation of about 20 degrees. Here, the effects of loss of control at high drift/randomizing ratios appear. The pointing statistics are more favorable, but at the cost of the target breaking constraints. Again, imagine the stick with a piece of string attached to each end as described in Chapter II. If one end of the string is loosened and required only to be near the end of the stick, that is equivalent to adding more string and thereby easing the constraints. When the mean square radial distance for Brownian-derived motion is

Table 4: Mean Angle (and Standard Deviation) in Degrees Between Present Course and Course from Present Position to Destination for Brownian-derived Motion (Three Values of Sigma Square) and Random Tour with Drift

sigma square		V_d/V_r = 2.69	1.13	1.0	0.58	0.26	0.126
1	mean	55.58	56.01	55.52	61.62	75.52	83.07
	std.dev.	15.05	16.72	16.59	28.12	44.45	48.91
5	mean	55.82	56.69	56.61	62.79	75.04	82.80
	std.dev.	20.22	24.19	25.50	34.76	45.69	49.73
10	mean	56.49	58.25	57.63	65.13	76.71	83.37
	std.dev.	24.34	28.82	30.43	38.02	47.02	50.14
rand. tour	mean	13.82	38.49	44.28	69.98	84.81	85.32
	std.dev.	6.94	20.40	27.25	47.38	50.44	52.22

examined, the lack of control at high drift/randomizing ratios will become evident.

3. The pointing statistics show that for Brownian-derived motion lower values of σ_2 produce slightly more pointing. This phenomenon is most pronounced at high V_d/V_r ratios, where the process is not under control anyway. However, it demonstrates that even at the same ratio, a smaller variance for the position sampling causes the process to be more constrained. The slight difference in statistics would most likely be greater if low variance legs were not extended more and clipped less than high variance ones.
4. The histograms in Figures 9a-c show that the standard deviations of the distibutions tend to increase and decrease with the means. The low mean distributions are peakier than the high mean ones, indicating processes that are more constrained; the opposite is true of less constrained paths.

The third and final measure of effectiveness for Brownian-derived motion is the mean square radial distance between present position and baseline position, measured periodically throughout path generation so that a graph or set of ordered pairs $(t, E[R_{t2}])$ is produced for comparison with other path generation methods. Significant results for this measure are:

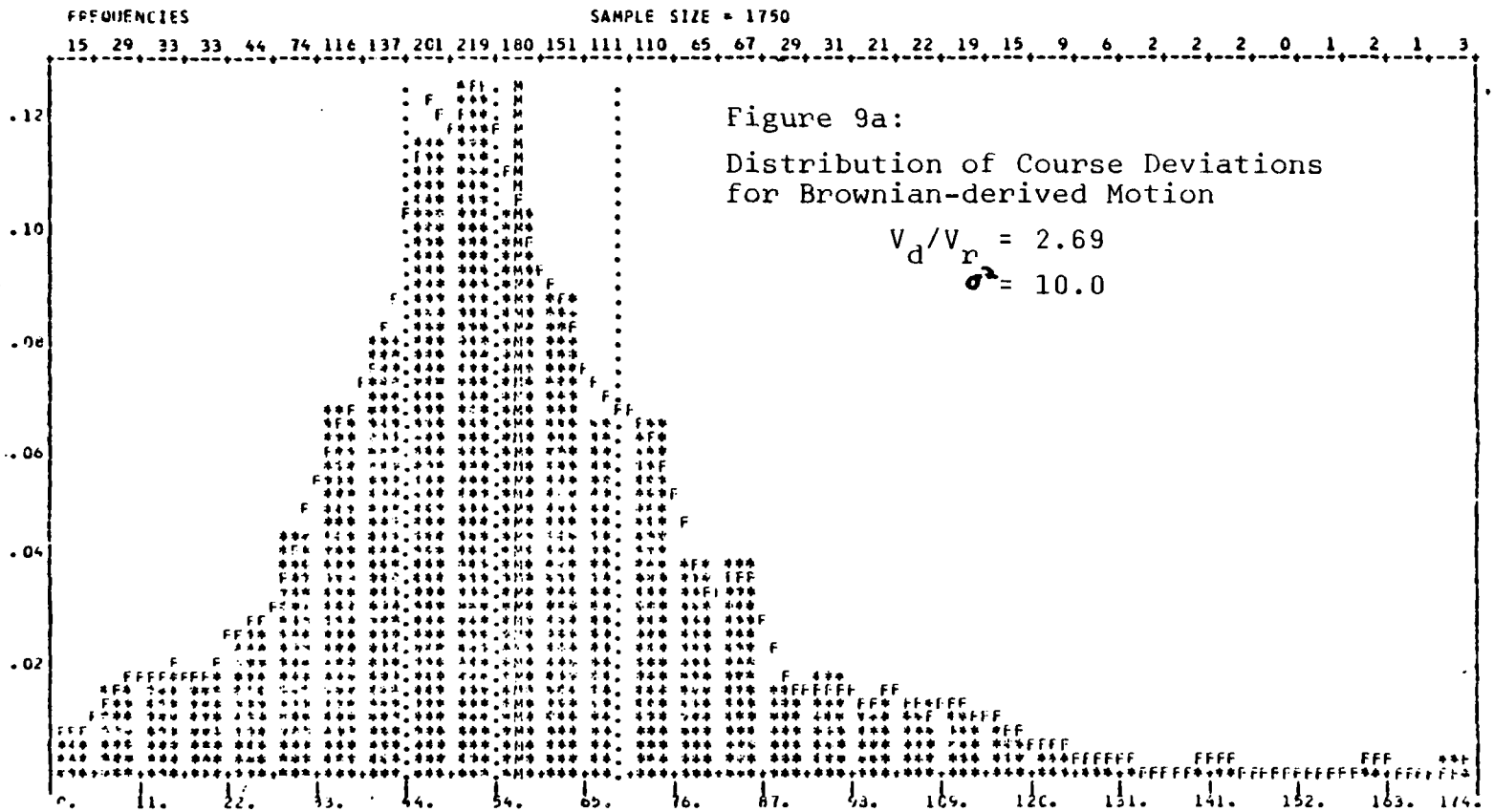

Figure 9a:

Distribution of Course Deviations for Brownian-derived Motion

$V_d/V_r = 2.69$

$\sigma^2 = 10.0$

CENTRAL TENDENCY		SPREAD		HIGHER CENTRAL MOMENTS		DISTRIBUTION	
MEAN	5.[illegible]9330E+01	VARIANCE	5.923916E+02	M3	1.103209E+04	MINIMUM	8.101940E-02
MEDIAN	5.258362E+01	STD DEV	2.433910E+01	M4	1.665389E+06	.10 QUANTILE	2.907211E+01
TRIMEAN	5.433156E+01	COEF VAR	4.308544E-01	SKEWNESS	7.651465E-01	.25 QUANTILE (HINGE)	4.221237E+01
MIDMEAN	5.445885E+01	MEAN DEV	1.800186E+01	KURTOSIS	1.802666E+00	.50 QUANTILE (MEDIAN)	5.258362E+01
MIDRANGE	8.705951E+01	RANGE	1.739570E+02	BETA1	1.101318E+04	.75 QUANTILE (HINGE)	6.674661E+01
GEOMEAN	4.996266E+01	MIDSPREAD	2.653424E+01	BETA2	1.682738E+06	.90 QUANTILE	8.622530E+01
HARMEAN	2.695689E+01					MAXIMUM	1.740380E+02

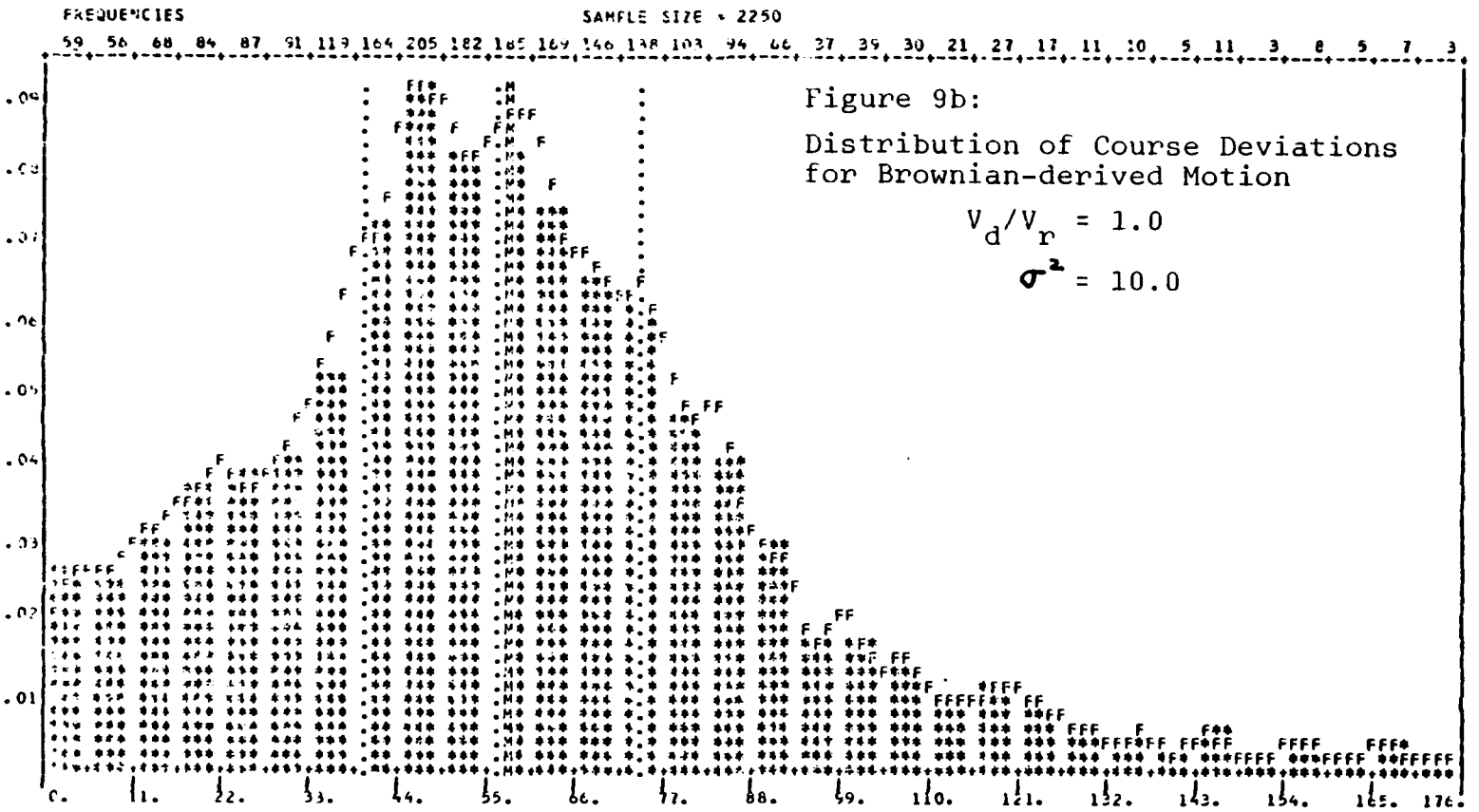

Figure 9b:

Distribution of Course Deviations for Brownian-derived Motion

$V_d/V_r = 1.0$

$\sigma^2 = 10.0$

CENTRAL TENDENCY		SPREAD		HIGHER CENTRAL MOMENTS		DISTRIBUTION		
MEAN	5.762842E+01	VARIANCE	9.257078E+02	M3	1.9932224E+04	MINIMUM		3.634644E-02
MEDIAN	5.537904E+01	STD DEV	3.042545E+01	M4	3.4458108E+06	.10 QUANTILE		1.952018E+01
TRIMEAN	5.585767E+01	COEF VAR	5.279590E-01	SKEWNESS	7.076938E-01	.25 QUANTILE	(HINGE)	3.647386E+01
MIDMEAN	5.561525E+01	MEAN DEV	2.311729E+01	KURTOSIS	1.021088E+00	.50 QUANTILE	(MEDIAN)	5.537904E+01
MIDRANGE	8.752500E+01	RANGE	1.750961E+02	BETA1	1.900096E+04	.75 QUANTILE	(HINGE)	7.433842E+01
GEOM MEAN	5.673277E+01	MIDSPREAD	3.786487E+01	BETA2	3.441967E+06	.90 QUANTILE		9.477241E+01
HARM MEAN	5.581095E+01					MAXIMUM		1.77[illegible]E+02

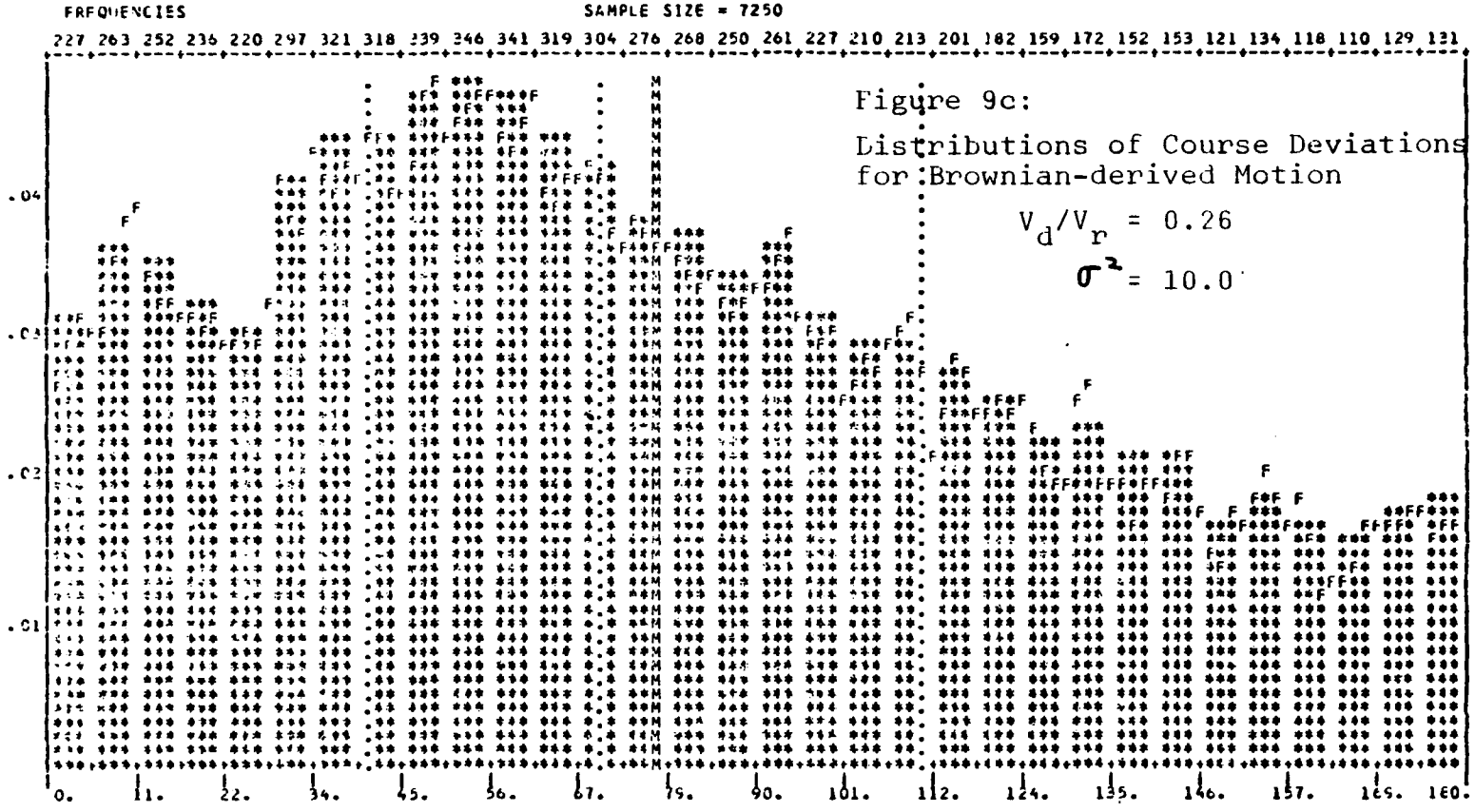

Figure 9c:

Distributions of Course Deviations for Brownian-derived Motion

$V_d/V_r = 0.26$

$\sigma^2 = 10.0$

CENTRAL TENDENCY		SPREAD		HIGHER CENTRAL MOMENTS		DISTRIBUTION	
MEAN	7.671262E+01	VARIANCE	2.211556E+03	M3	3.902191E+04	MINIMUM	2.471924E-03
MEDIAN	7.036293E+01	STD DEV	4.702718E+01	M4	1.071931E+07	.10 QUANTILE	1.435349E+01
TRIMEAN	7.295851E+01	COEF VAR	6.130355E-01	SKEWNESS	3.751992E-01	.25 QUANTILE (HINGE)	3.530206E+01
MIDMEAN	7.199921E+01	MEAN DEV	3.909709E+01	KURTOSIS	-8.083506E-01	.50 QUANTILE (MEDIAN)	7.006253E+01
MIDRANGE	8.502332E+01	RANGE	1.759617E+02	BETA1	3.900579E+04	.75 QUANTILE (HINGE)	1.105657E+02
GEOM MEAN	5.686450E+01	MIDSPREAD	7.166307E+01	BETA2	1.071745E+07	.90 QUANTILE	1.477077E+02
HARM MEAN	9.191649E+00					MAXIMUM	1.755044E+02

1. Figures 10a-d illustrate mean square radial distance for four V_d/V_r ratios and $\lambda = 1.0$; each figure has curves for three different values of the physical parameter σ_2. Immediately it is clear that the mean square radial distance decreases as the drift/randomizing ratio increases. This result follows directly from the greater constraint placed on the target at higher ratios, and is similar to the results for the random tour with drift.

2. The problem of control for Brownian-derived motion is apparent in these figures. Even in Figures 10a and 10b, at the lowest two drift/randomizing ratios, the mean square radial distance does not go down to zero, indicating that on the average the target does not visit the destination. Notice that as the ratio becomes progressively higher in Figures 10c and 10d that the mean square radial distance tends to become even greater at the end of the time period. Clearly, as the problem becomes more constrained, control is lost. Another characteristic of this path generating method with small lambda is the hook in the curve at the end of the time period, indicating an undesireable increase in mean square radial distance during the final time unit of travel. This increase is the result of the truncation of the final leg when time runs out, though the random numbers for the final leg were generated as

Figure 10a:

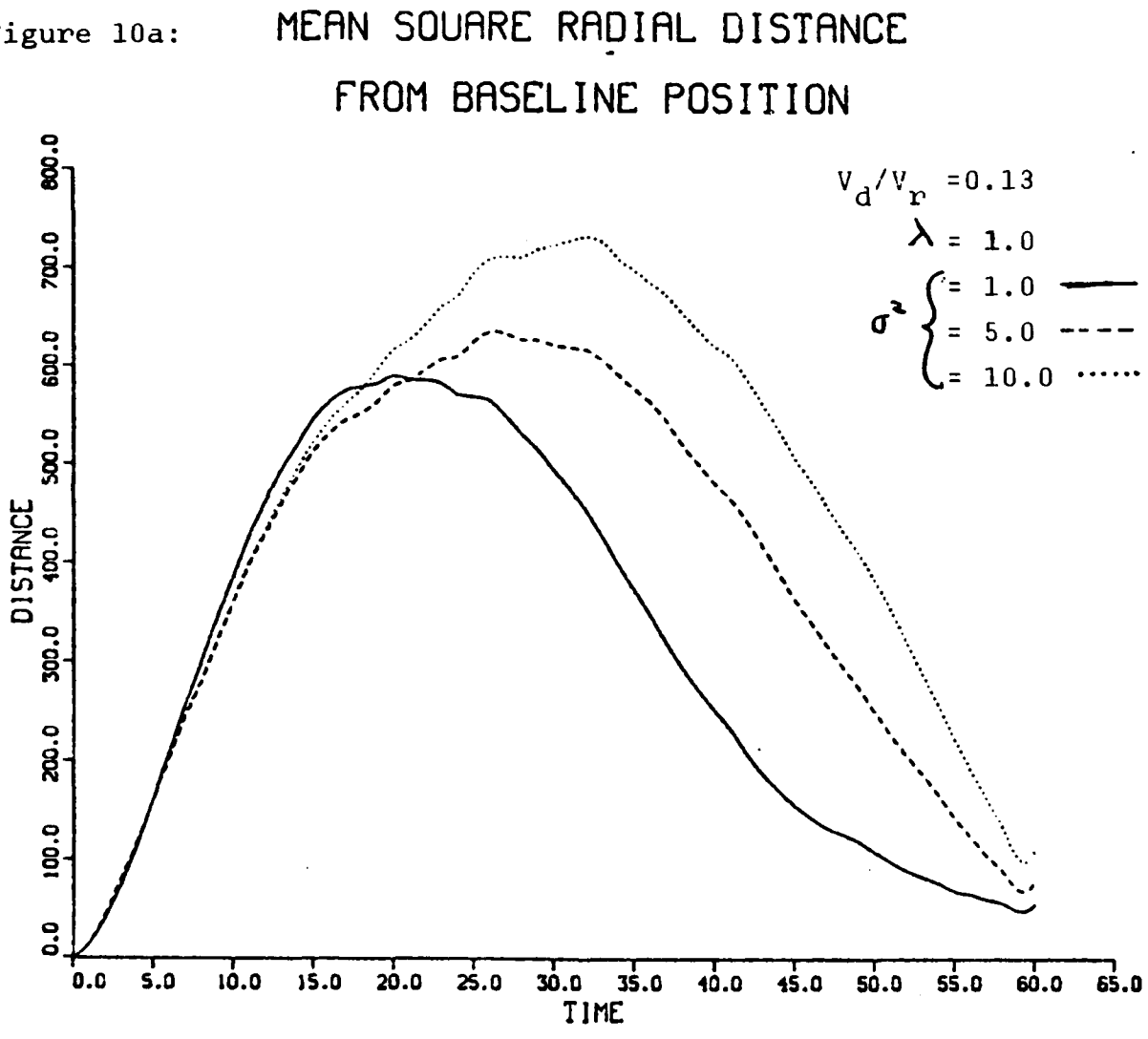
MEAN SQUARE RADIAL DISTANCE
FROM BASELINE POSITION
V_d/V_r =0.13
λ = 1.0
σ^2 = 1.0
= 5.0
= 10.0
DISTANCE
0.0
100.0
200.0
300.0
400.0
500.0
600.0
700.0
800.0
0.0
5.0
10.0
15.0
20.0
25.0
30.0
35.0
40.0
45.0
50.0
55.0
60.0
65.0
TIME

Figure 10b: MEAN SQUARE RADIAL DISTANCE FROM BASELINE POSITION

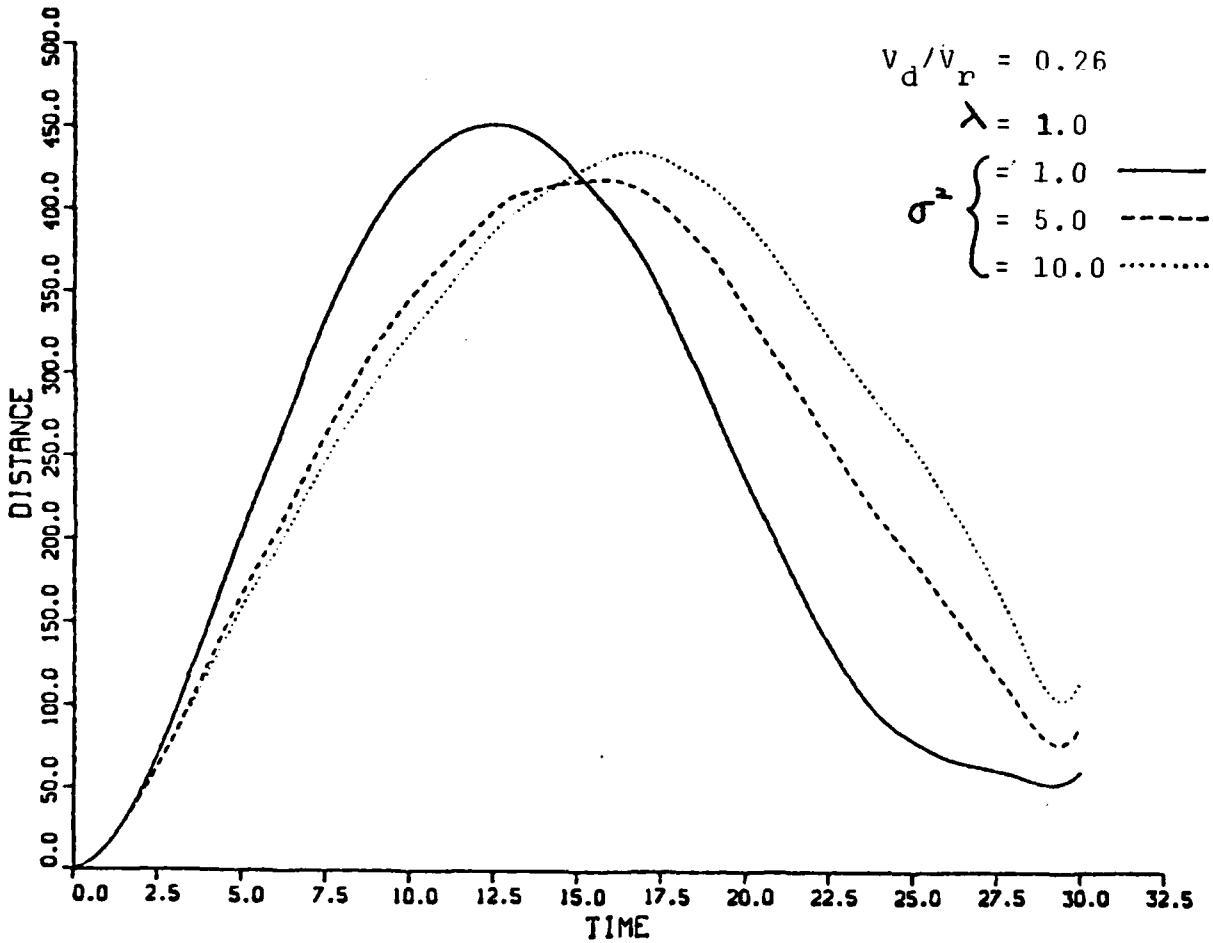

Figure 10c:

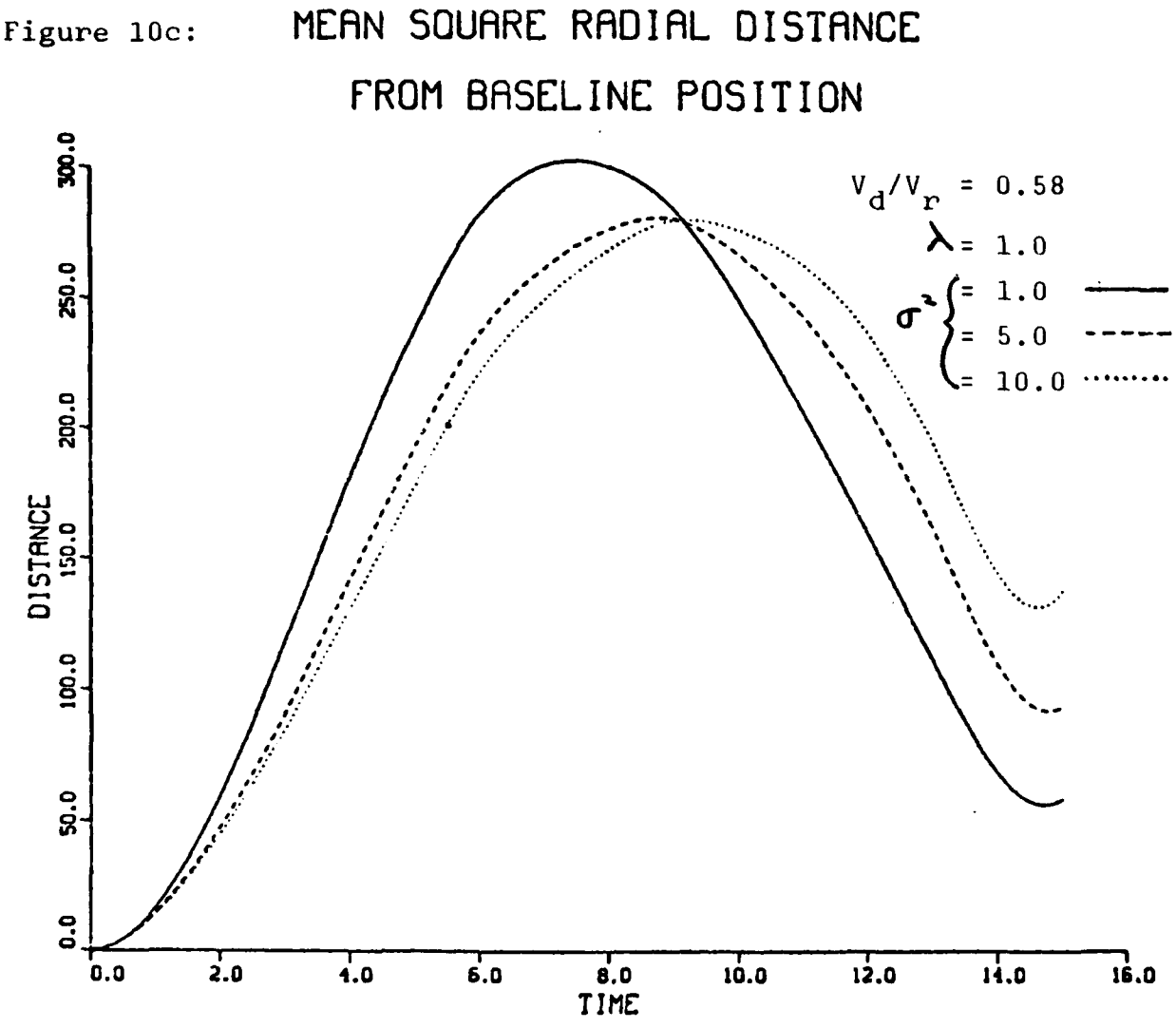
MEAN SQUARE RADIAL DISTANCE
FROM BASELINE POSITION
V_d/V_r = 0.58
λ = 1.0
σ^2 = 1.0
= 5.0
= 10.0
DISTANCE
0.0
50.0
100.0
150.0
200.0
250.0
300.0
0.0
2.0
4.0
6.0
8.0
10.0
12.0
14.0
16.0
TIME

Figure 10d:

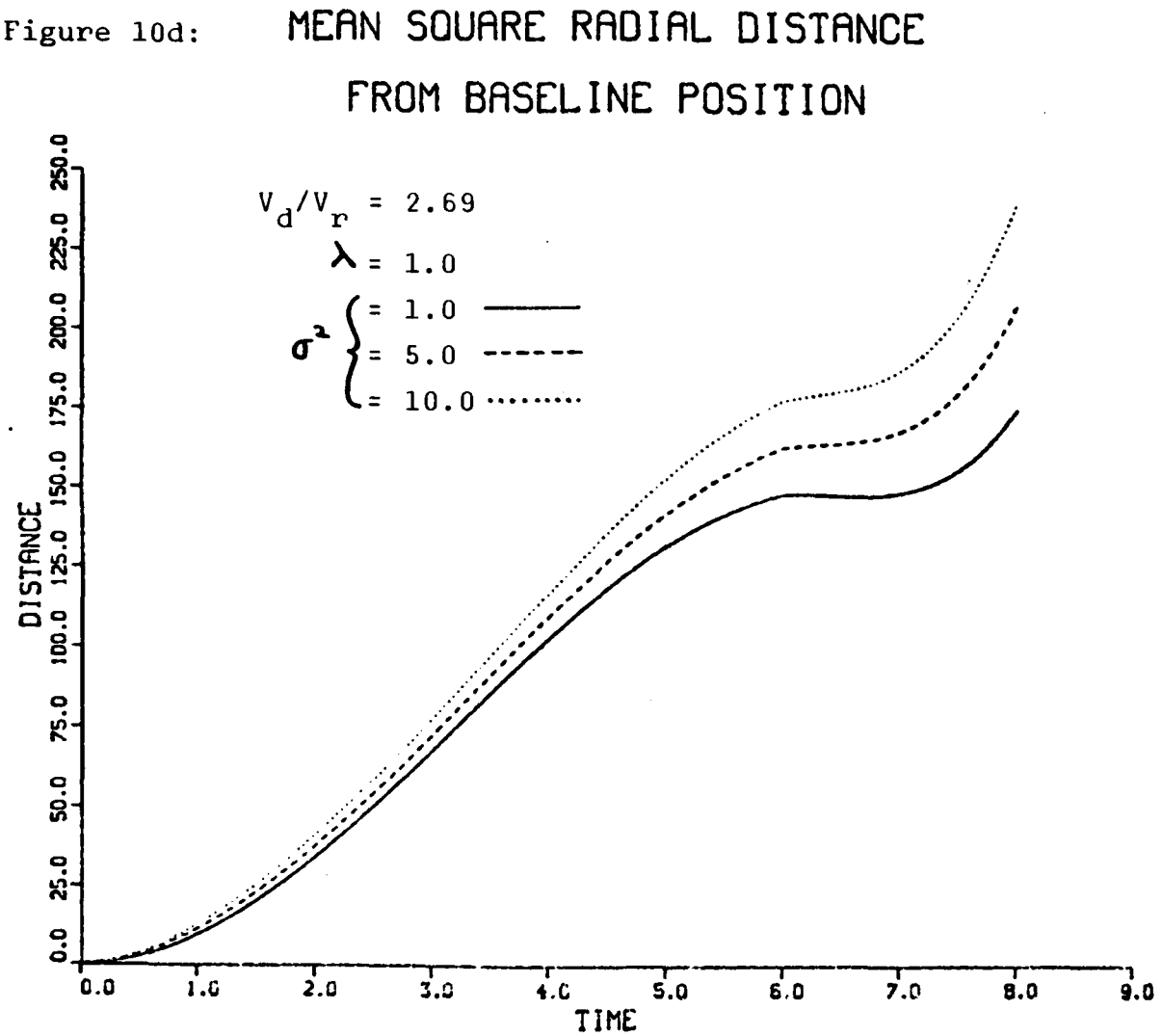
MEAN SQUARE RADIAL DISTANCE
FROM BASELINE POSITION
V_d/V_r = 2.69
λ = 1.0
σ^2 = 1.0
= 5.0
= 10.0
DISTANCE
0.0
25.0
50.0
75.0
100.0
125.0
150.0
175.0
200.0
225.0
250.0
TIME
0.0
1.0
2.0
3.0
4.0
5.0
6.0
7.0
8.0
9.0

if no truncation takes place. The simple solution is for the target to travel directly toward the destination on the last leg in order to get as close as possible. A target would probably do that anyway since it does not really need to be told what to do on the final leg. The algorithm for path generation was purposely not modified in order to demonstrate this peculiar phenomenon. However, it is important to realize that a true "bridge", Brownian or otherwise, does not exist as long as the two endpoints are not connected by the target path.

3. At lower drift/randomizing ratios, the mean square radial distance is less for smaller σ_2, as Figure 10a clearly illustrates. However, as the ratio increases, the mean square radial distance is approximately the same for all three values of σ_2. The curves in Figures 10b-d also show that for different σ_2 values the maximum mean square radial distance occurs at different times for a given drift/randomizing ratio. The mean square radial distances for different σ_2 become closer in value because of the clipping and entending process that occurs to keep the target within speed limits. As the problem becomes more constrained at higher drift/randomizing ratios, the target tends to bump into the speed bounds more. Hence, the process is clipped and extended more and the natural differences among the σ_2

values dominate less than the speed limits, which all paths must obey equally. Also, as the mean square radial distances for various sigma square all get closer to the baseline for whatever reason, they are bounded on one side by the baseline (the minimum value) and get sandwiched together, as Figure 10d clearly demonstrates.

4. Figures 10a-d show that for a given V_d/V_r there is a value of sigma square which produces a mean square radial distance curve that is symmetrical about the line $x = T/2$. For Figures 10a-c the values of sigma square which come closest to symmetry are 10, 5, and 1 respectively. Notice also, that in Figures 10a and 10b, in which the drift/randomizing ratios are low and sigma square equal to ten and five are the values closest to producing symmetry, the curve for sigma square equal to one is very asymmetrical and flattens out for big t. This occurs because for these low drift/randomizing ratios, $\sigma_2 = 1$ over-constrains the process; it forces the target back to the baseline too soon.

5. Figures 11a-d are different from Figures 10a-d only in their lambda value which is 3.0 instead of 1.0. It is immediately clear that an increase in lambda causes a marked decrease in mean square radial distance. A similar result was found for the random tour, for which

an increase in lambda caused the distribution of radial distance to start piling up around the expected position of the process. There are some other subtle differences also. At low V_d/V_r ratios, all curves for the three sigma square values are skewed slightly less left than for higher lambda, and for higher drift/randomizing ratios they are skewed slightly more right. Notice also that the curves for the lowest drift/randomizing ratio in Figure 11a are closer together than they were for the same ratio at $\lambda = 1.0$ in Figure 10a. This, again, is the result of all curves being bound on one side by the baseline, and therefore forced together more at the lower mean square radial distances which higher lambda produces. Finally, the "hook" on the end of the curves is gone, most likely because the mean number of turns during the final time unit is three instead of one. Consequently, the target turns a few more times during the last time unit of travel toward the destination and thus does not rely only on one leg to hit or miss. Again, however, it is likely that a target would travel directly to destination at this point anyway, unless it desired to adhere to its course change policy strictly.

Figure 11a: MEAN SQUARE RADIAL DISTANCE FROM BASELINE POSITION

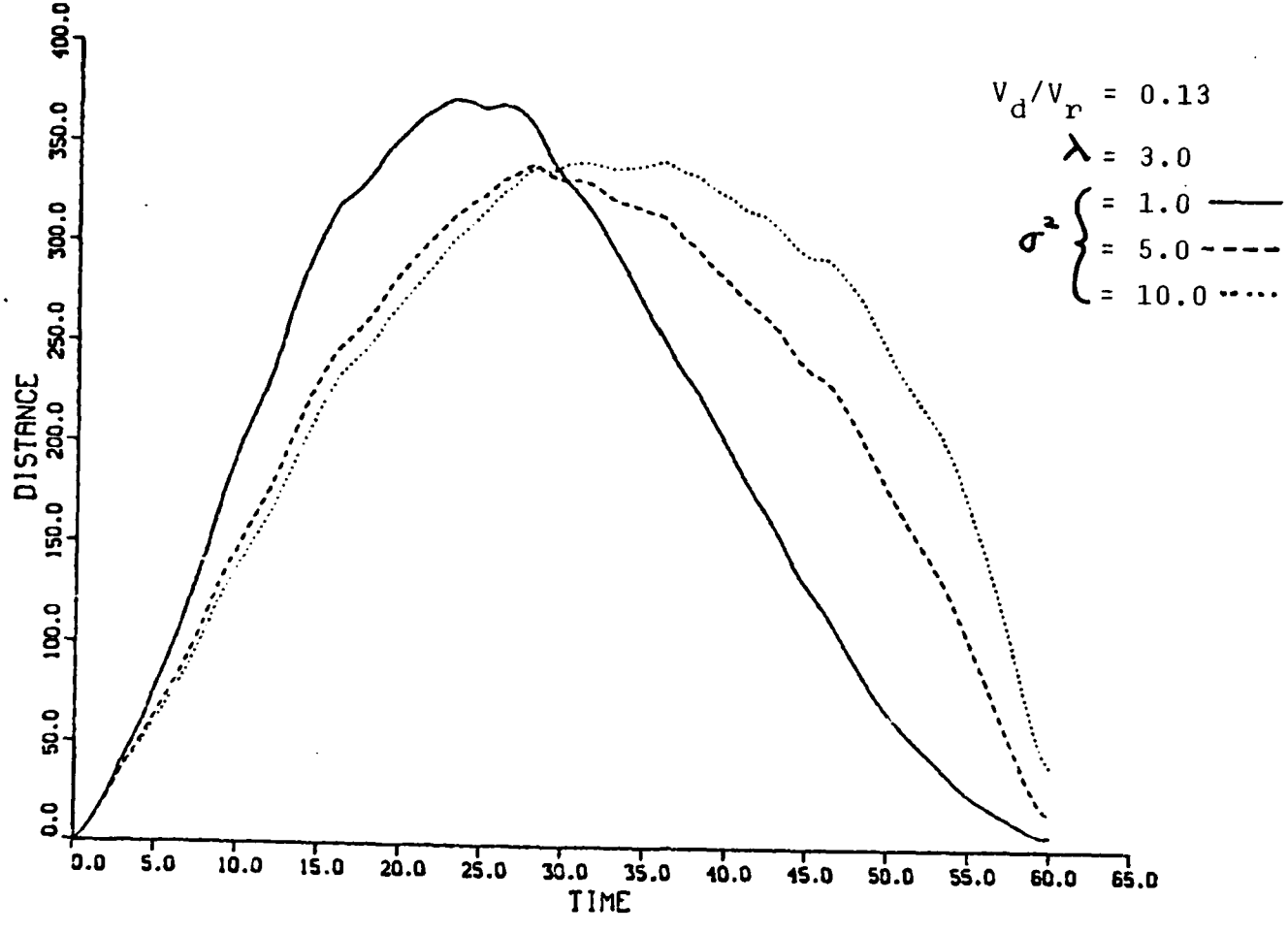

Figure 11b: MEAN SQUARE RADIAL DISTANCE FROM BASELINE POSITION

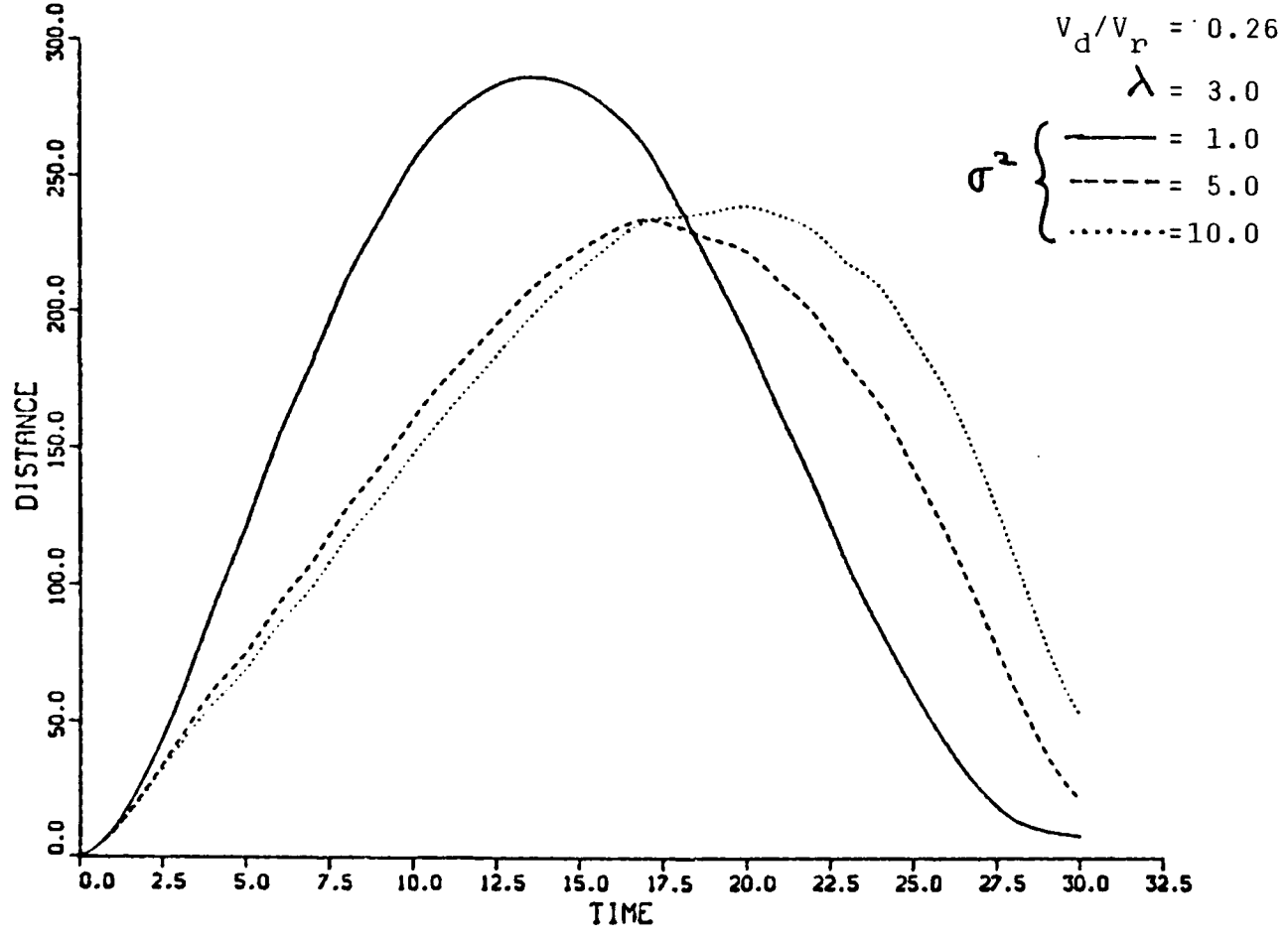

AD-A127 805 TWO MODELS OF TIME CONSTRAINED TARGET TRAVEL BETWEEN TWO ENDPOINTS CONSTR.. (U) NAVAL POSTGRADUATE SCHOOL MONTEREY CA W J COMSTOCK MAR 83 2/2

UNCLASSIFIED F/G 12/1 NL

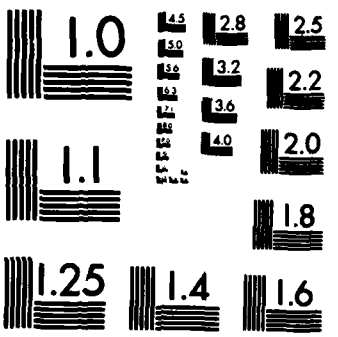

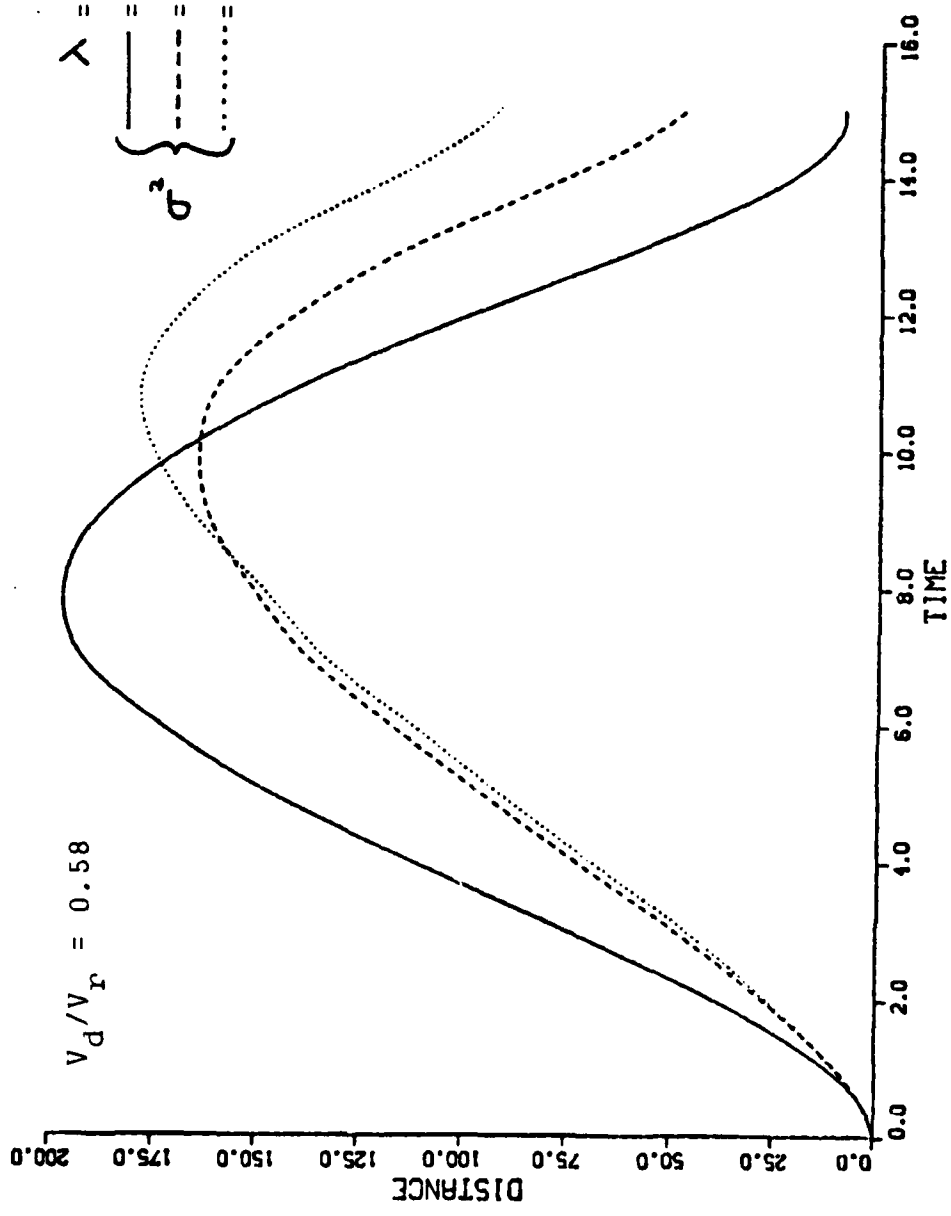
MEAN SQUARE RADIAL DISTANCE
FROM BASELINE POSITION
V_d/V_r = 0.58
σ^2
λ = 3.0
= 1.0
= 5.0
= 10.0
DISTANCE
TIME
0.0
25.0
50.0
75.0
100.0
125.0
150.0
175.0
200.0
2.0
4.0
6.0
8.0
10.0
12.0
14.0
16.0

Figure 11c:

Figure 11d: MEAN SQUARE RADIAL DISTANCE FROM BASELINE POSITION

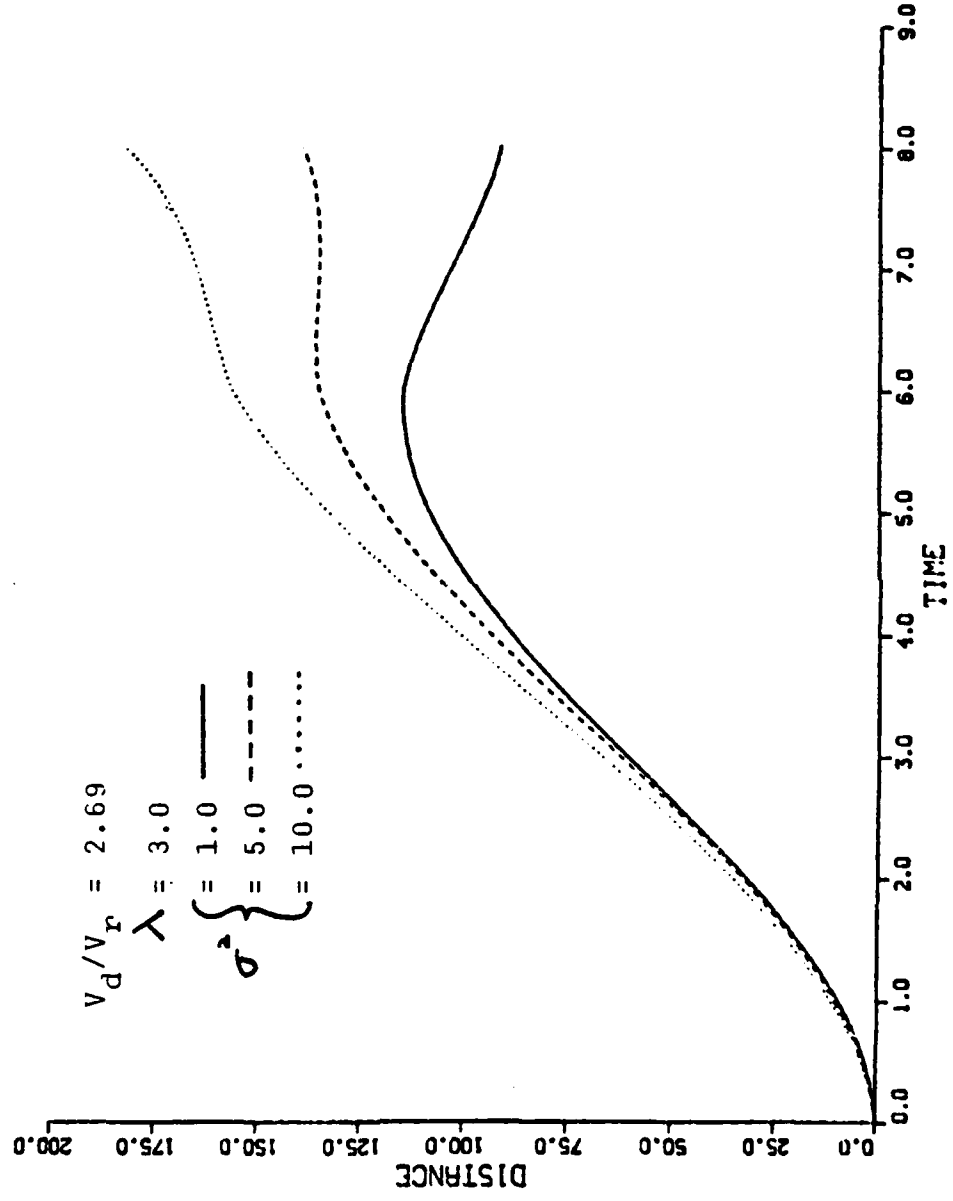

VI. CONCLUSIONS

Chapter I defined a controlled time of arrival scenario in which a time constraint is placed on a target that is required to travel between two endpoints. It is desireable for the target to "randomize" its motion during the transit in order to provide the enemy with as little information as possible about target origin and destination and to make target detection and redetection difficult. Chapter II discussed desireable qualities for such target travel and delineated three measures of effectiveness against which to measure any procedure for producing target paths, and Chapter III examined previous investigations into the problem which have provided direction for the two approaches adopted in this thesis. Chapter IV described the random tour with drift and discrete Brownian-dervied motion in detail, and while the results for each method were presented in Chapter V, the performance of a path producing procedure against the measures of effectiveness is not important in itself; but rather, the measures provide a way to compare two or more procedures, one of which can be judged best for a particular situation.

The amount a target points away from orign or to destination is very nearly the same for both the random tour with drift and discrete Brownian-derived motion. Tables 1

and 4, which list the mean values and standard deviations of the course deviation distributions, show nearly identical values for both procedures at low V_d/V_r ratios. Differences begin to show only as the ratio gets bigger. But though the statistics become more favorable for Brownian-derived motion, it is probably because that process is not under complete control of the constraints when the drift/randomizing ratio is high. If it were completely controlled or if the random tour were also allowed to violate the final visitation constraint, then the statistics would probably be very nearly identical over the whole range of V_d/V_r ratios.

The failure of Brownian-derived motion to control target travel by guaranteeing visitation on time at the destination is a potential weakness of the process; it literally does not do exactly what it is supposed to do. However, the weakness is not important just as long as it is not vital for the target to get <u>exactly</u> to destination <u>exactly</u> on time. If it is vital, then clearly the choice is in favor of the random tour, and none of the measures of effectiveness are relevant, except for the requirement that the path "look good" and be executable as described in Chapter II.

If the target does not need to have a perfectly controlled time of arrival, and can either fall short of its destination at the appointed time or else take extra time to get there, then the mean square radial distance becomes the important measure of effectiveness; pointing to origin and

destination is similar and representative paths of both procedures "look good" and are executable. Figures 12a-d illustrate the mean square radial distance between present and baseline positions for two sigma square values of Brownian-derived motion and for the random tour with drift with and without the requirement for the left and right paths to match. While the mean square radial distances for random tour paths which do not match have no practical significance since such paths meet none of the constraints, they do show how much radial distance is lost by requiring that the left and right paths meet. Recall that the loss is about two per cent per time unit, and while that sounds low, it is becomes very significant as time progresses. The figure of two percent was obtained, as previously described, by linear regression and is valid only over the range of time for which the regression was done. This limitation is illustrated in Figures 12a and 12b. Notice that the curve for matching random tour paths begins to sag in the middle, when actually the mean square radial distance should be increasing, however slightly. The sagging is a direct result of the linear regression operating at the edge of its valid range. The curve should be rather flatly rounded in the middle instead of sagging. However, the curves presented are accurate over their range, with the exception of the slight sagging as described. In Figures 12c and 12d, where the time period is shorter, the curves do not sag at all. Most importantly, all

Figure 12a:

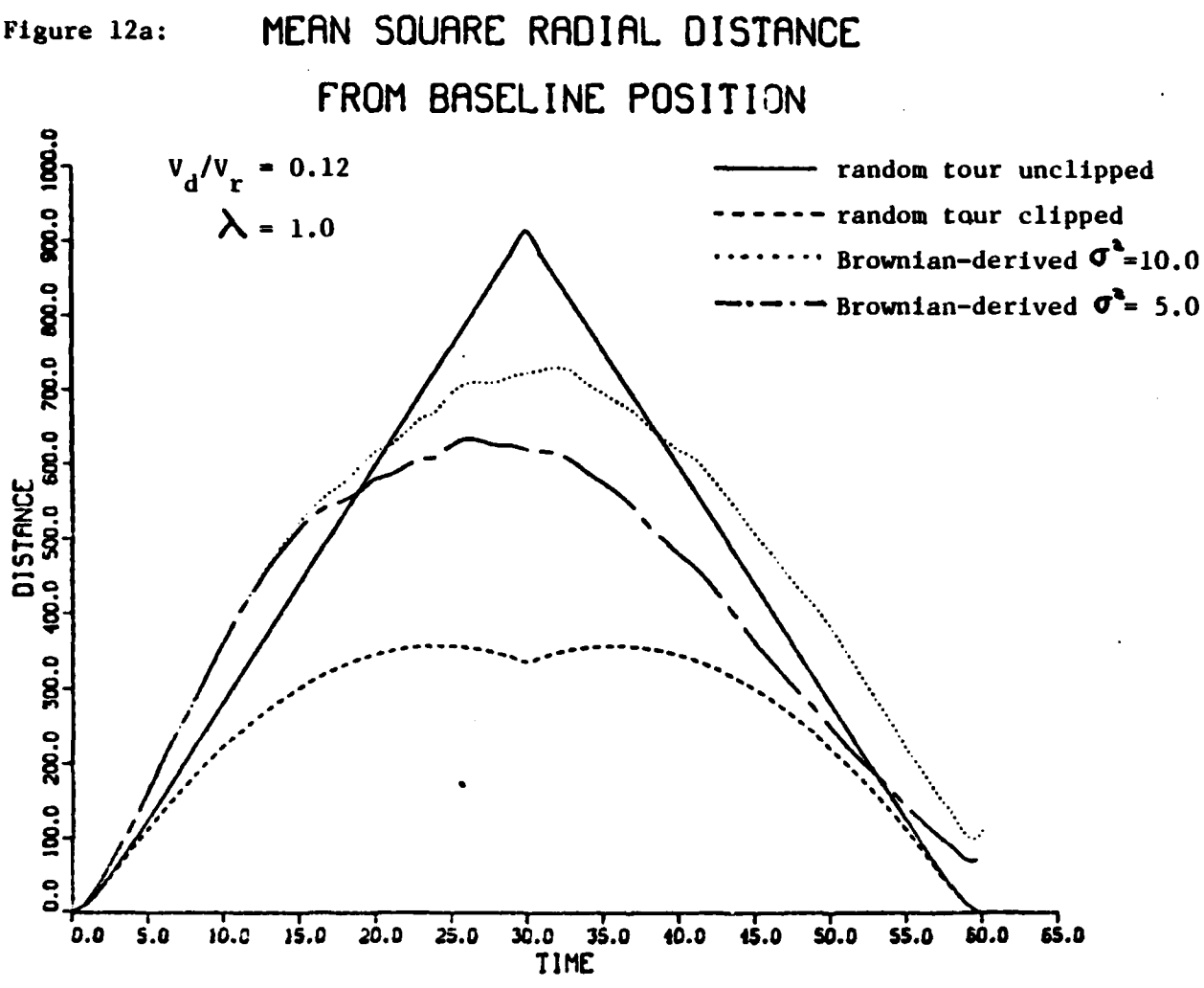
MEAN SQUARE RADIAL DISTANCE
FROM BASELINE POSITION
V_d/V_r = 0.12
λ = 1.0
random tour unclipped
random tour clipped
Brownian-derived σ^2=10.0
Brownian-derived σ^2= 5.0
DISTANCE
0.0
100.0
200.0
300.0
400.0
500.0
600.0
700.0
800.0
900.0
1000.0
TIME
0.0
5.0
10.0
15.0
20.0
25.0
30.0
35.0
40.0
45.0
50.0
55.0
60.0
65.0

Figure 12b:

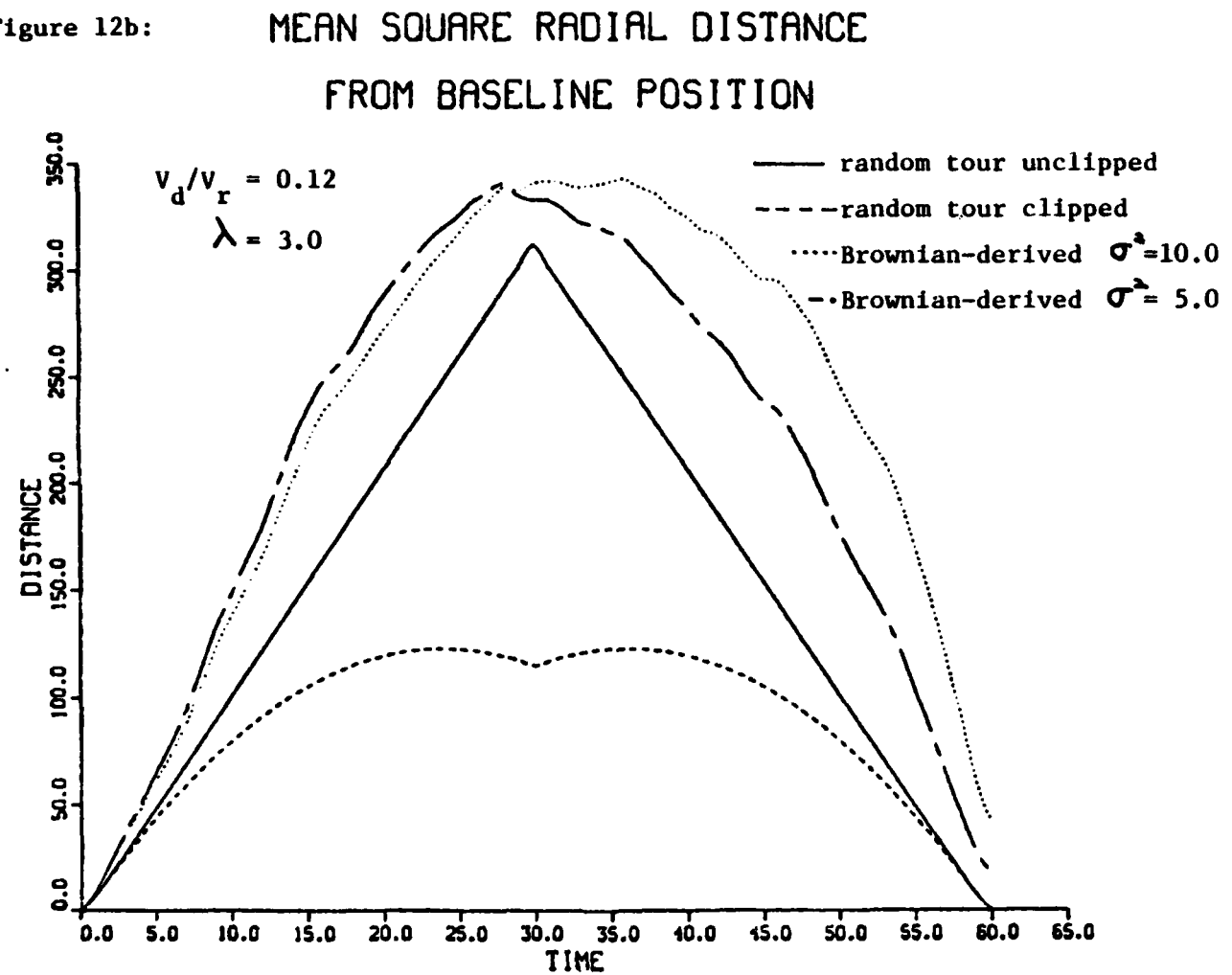
MEAN SQUARE RADIAL DISTANCE
FROM BASELINE POSITION
V_d/V_r = 0.12
λ = 3.0
random tour unclipped
random tour clipped
Brownian-derived σ^2=10.0
Brownian-derived σ^2= 5.0
DISTANCE
0.0
50.0
100.0
150.0
200.0
250.0
300.0
350.0
0.0 5.0 10.0 15.0 20.0 25.0 30.0 35.0 40.0 45.0 50.0 55.0 60.0 65.0
TIME

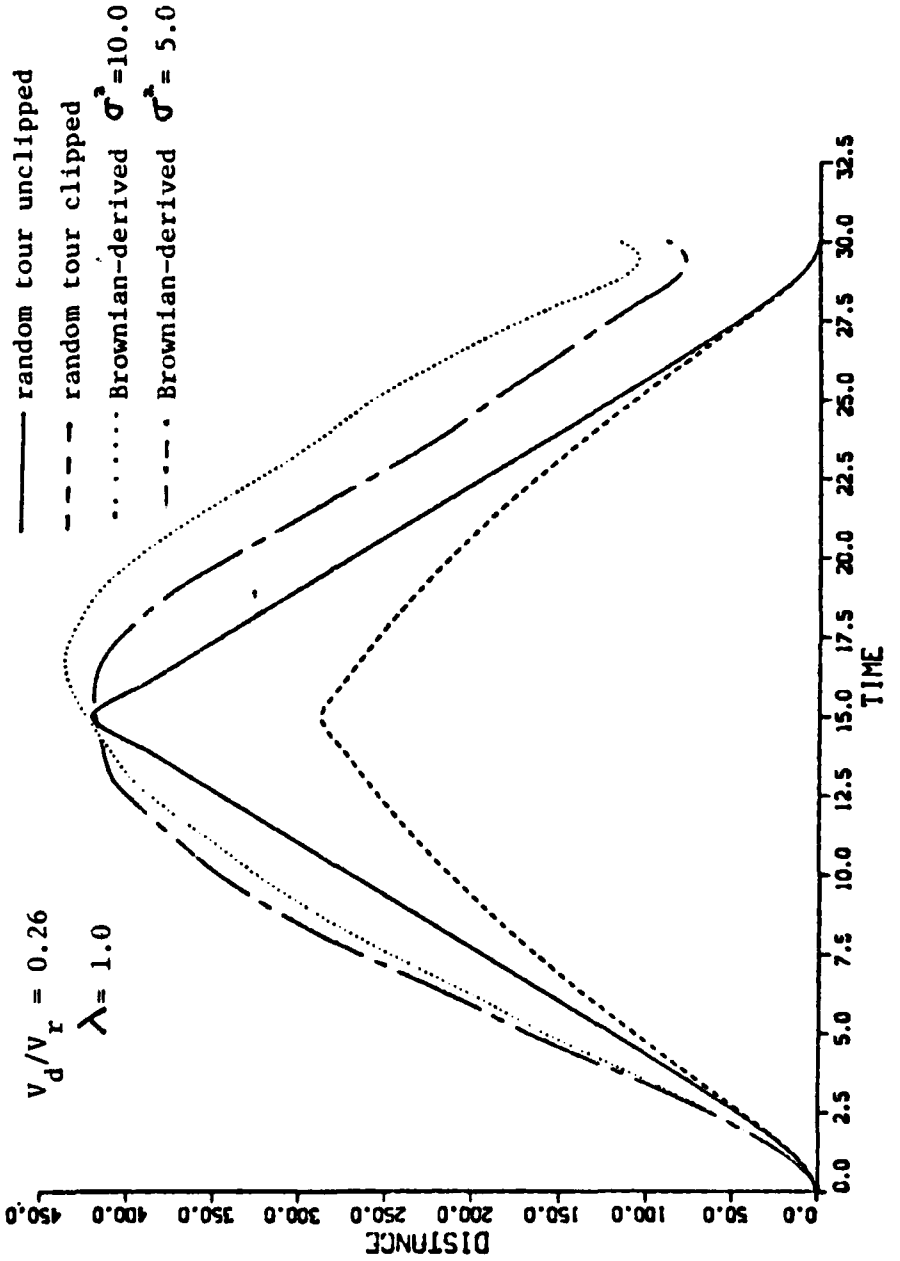
MEAN SQUARE RADIAL DISTANCE
FROM BASELINE POSITION
random tour unclipped
random tour clipped
Brownian-derived σ^2=10.0
Brownian-derived σ^2= 5.0
V_d/V_r = 0.26
λ= 1.0
DISTANCE
TIME
0.0
50.0
100.0
150.0
200.0
250.0
300.0
350.0
400.0
450.0
0.0
2.5
5.0
7.5
10.0
12.5
15.0
17.5
20.0
22.5
25.0
27.5
30.0
32.5

Figure 12c:

Figure 12d:

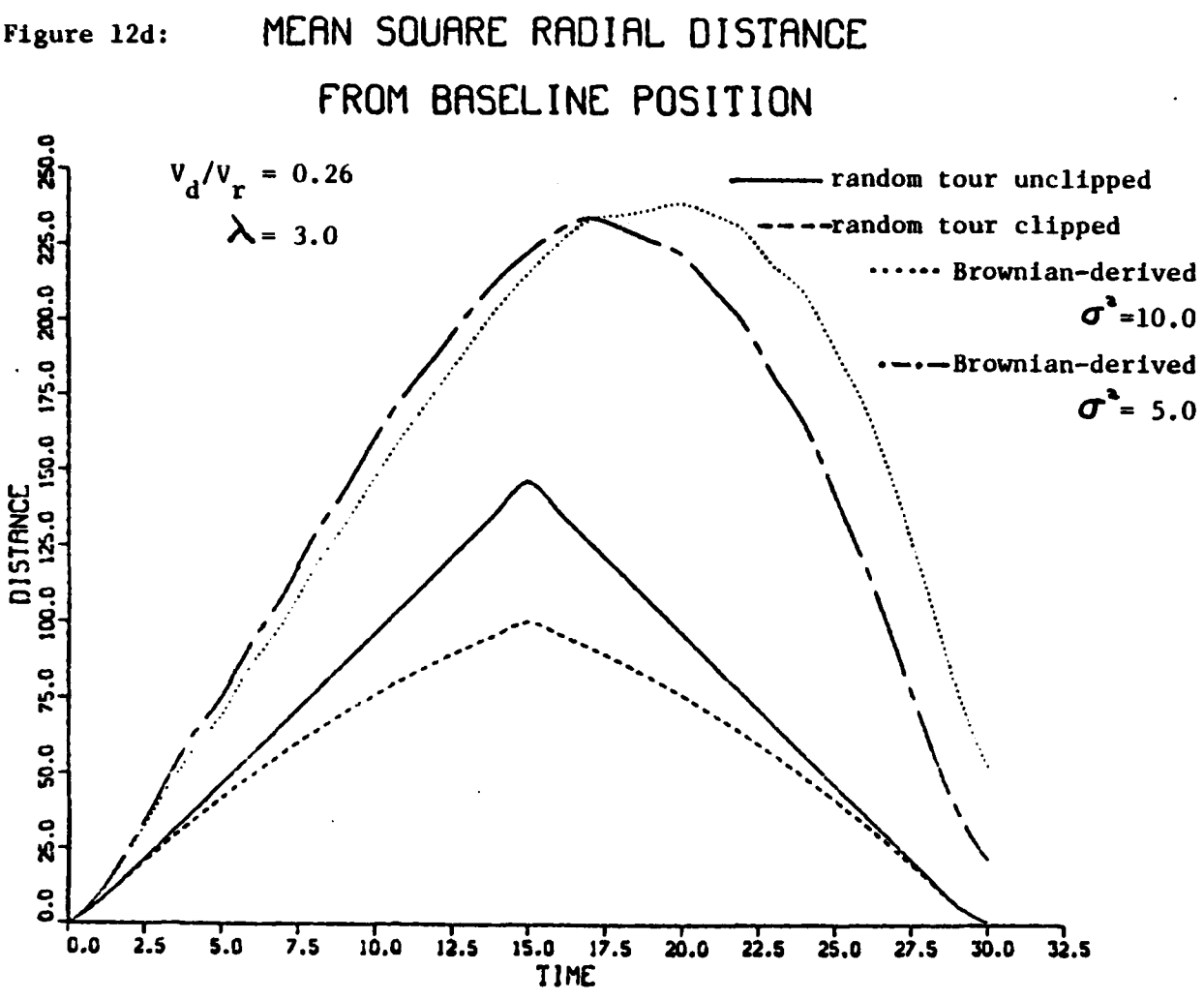
MEAN SQUARE RADIAL DISTANCE
FROM BASELINE POSITION
V_d/V_r = 0.26
λ = 3.0
random tour unclipped
random tour clipped
Brownian-derived
σ^2=10.0
Brownian-derived
σ^2= 5.0
DISTANCE
0.0
25.0
50.0
75.0
100.0
125.0
150.0
175.0
200.0
225.0
250.0
TIME
0.0
2.5
5.0
7.5
10.0
12.5
15.0
17.5
20.0
22.5
25.0
27.5
30.0
32.5

four figures show how much mean square radial distance is lost by requiring the paths to match. Under the conditions prevailing in Figure 12a, the unconstrained random tour with drift exhibits a greater mean square radial distance than Brownian-derived motion does for either sigma square value. However, the mean square radial distances for the matching random tour paths are much less than those for Brownian-dervived motion in all figures. Notice also that while an increase in the v_d/v_r ratio or lambda each cause a reduction in mean square radial distance for both procedures, that increasing lambda affects the random tour process much more adversely than Brownian-derived motion. This is a point in favor of the Brownian-derived process.

One might argue that it is natural for Brownian-derived motion to exhibit higher mean square radial distances, if only because the process is not under control. This argument is not compelling and one need only to look at the figures to see the great disparity. It is not likely that the failure of the mean square radial distance for Brownian motion to go all the way to zero at the destination is the reason that it is more than double that of the random tour in the midrange for three of the four cases. However, one might argue further that the constraint which requires the left and right random tour paths to meet up causes such severe degradation, and that Brownian motion might suffer similarly if it could be made to meet the constraints exactly. Nonetheless, the

paths perform differently as they are, and clearly the mean square radial distances are much more favorable for Brownian-derived motion if the strict breaking of the final visitation constraint can be tolerated, and remedied.

Recall that the first measure of effectiveness which is applied to a path producing procedure checks representative paths to see whether they "look good" and are executable by a candidate target. Failure against this measure automatically disqualifies a path from further consideration. While both the random tour with drift and Brownian-derived motion passed this vital first test, there is a subtlety in the way both procedures are executed that makes Brownian-derived motion more desireable. In order to obtain matching left and right paths, the random tour must be executed in its entirety before the target begins a journey. The target must then follow the instructions closely to make all the correct courses and turns. While this procedure is possible to carry out, it is quite exacting. On the other hand, Brownian-derived motion can be executed one leg at a time because after each leg the controlled time of arrival problem is reframed as a totally new one using present position as the new origin. Hence, perfect navigation is not as critical as it is for the random tour. In a sense, starting the process over after each leg always gives the target another chance, just so long as a flagrant violation does not occur which causes the target to be faced with an impossible transit at

the beginning of some intermediate leg. This feature of Brownian-derived motion should make it more saleable to target captains.

Both methods for producing paths should be available for a target to choose. Clearly, if the final visitation constraint absolutely must be met on time, then the random tour with drift method provides the only guarantee. But, if the target needs only to ensure that it arrives in the immediate vicinity of the destination or may arrive at the actual destination slightly early or late, then discrete Brownian-derived motion performs more favorably against the selected measures of effectiveness and is easier for a target to execute.

The two very different methods presented here for generating paths represent only two among many, and the variations on these two procedures alones are infinite. For instance, the random tour with drift could be modified so that it was executed from one end only, instead of from both ends as done in this thesis. After each leg of travel the problem could be reframed as a totally new one, in much the same manner that Brownian-derived motion was restarted after each leg here. It is also quite possible, and desireable, to devise a way to force Brownian-derived motion to arrive at the destination exactly on time, satisfying all the constraints strictly. Thus, the two methods presented here

are not only quite workable, but also provide suggestions for further investigation.

LIST OF REFERENCES

1. Washburn, Alan, "Probability Density of a Moving Particle," Operations Reasearch, v. 17, no. 5, pp. 861-871, September-October 1969.

2. Daniel H. Wagner, Associates, Interim Memorandum to Applied Physics Laboratory/Johns Hopkins University, The Ornstein-Uhlenbeck Displacement Process as a Model of Target Motion, by Barry Belkin, Feb. 1, 1978.

3. Daniel H. Wagner, Associates, Interim Memorandum to Applied Physics Laboratory/Johns Hopkins University, The Random Tour Target Model with an Arbitrary Course Change Distribution, by Barry Belkin, July 27, 1979.

4. EPL Analysis, Random Walk Statistics, by Edward P. Loane, Nov. 4, 1977.

5. Daniel H. Wagner, Associates, Interim Memorandum to the Applied Physics Laboratory/Johns Hopkins University, RMS Velocity Behaviour of a Constrained IOU Process, by Barry Belkin, May 5, 1981.

6. Daniel H. Wagner, Associates, Interim Memorandum to Applied Physics Laboratory/Johns Hopkins University, The Random Tour Target Model with an Arbitrary Course Change Distribution, by Barry Belkin, p. 11, July 27, 1979.

7. Daniel H. Wagner, Associates, Interim Memorandum to the Applied Physics Laboratory/Johns Hopkins University, RMS Velocity Behaviour of a Constrained IOU Process, by Barry Belkin, p. 8, May 5, 1981.

8. Ibid, pp. 9-13.

9. Daniel H. Wagner, Associates, Interim Memorandum to the Applied Physics Laboratory/Johns Hopkins University, A Result Concerning Datum Aging, by Barry Belkin, Dec. 22, 1977.

10. Daniel H. Wagner, Associates, Interim Memorandum to the Applied Physics Laboratory/Johns Hopkins University, Error Analysis When Brownian Motion is Used as a Datum Aging Model, by Barry Belkin, Jan. 13, 1978.

11. Daniel H. Wagner, Associates, Interim Memorandum to Applied Physics Laboratory/Johns Hopkins University, The Ornstein-Uhlenbeck Displacement Process as a Model of Target Motion, by Barry Belkin, Feb. 1, 1978.

12. Ibid. p. 5.

13. Ibid, p.22.

14. Freedman, David A., Brownian Motion and Diffusion, p. 1, Holden-Day, 1971.

INITIAL DISTRIBUTION LIST

		No. Copies
1.	Defense Technical Information Center Cameron Station Alexandria, Virginia 22314	2
2.	Library, Code 0142 Naval Postgraduate School Monterey, California 93940	2
3.	Department Chairman, Code 55 Department of Operations Research Naval Postgraduate School Monterey, California 93940	1
4.	Dr. R. Neagle Forrest, Code 71 Naval Postgraduate School Monterey, California 93940	1
5.	Dr. Donald P. Gaver, Code 55gv Naval Postgraduate School Monterey, California 93940	4
6.	Dr. James N. Eagle, Code 55er Naval Postgraduate School Monterey, California 93940	1
7.	Dr. Kenneth V. Saunders Code 20231 Strategic Systems Project Office Washington, D.C. 20376	2
8.	Mr. John C. Sommerer Submarine Technology Systems Group Applied Physics Laboratory Johns Hopkins University Johns Hopkins Rd. Laurel, Maryland 20707	2
9.	LT W. Justin Comstock c/o Dr. Sidney O. Graves 110 Dana Rd. Natchez, Mississippi 39120	2